Volume 3 *December, 1932* *Number 6*

PHYSICS

The Theory of the Interpretation of Seismic Travel-Time Curves in Horizontal Structures

By L. B. SLICHTER
Massachusetts Institute of Technology
(Received August 31, 1932)

CONTENTS

Part I. NORMAL TYPE OF TIME-DISTANCE CURVE 274
1.1 Review of Herglotz-Wiechert solution 274
1.2 Validity of the solution above 277
Part II. A TRANSITIONAL CASE 278
2.1 A focus point as a discrete point 278
2.2 A focus point in a continuous travel-time curve 279
Part III. REVERSED TRAVEL-TIME CURVES 280
3.1 Condition for the occurrence of a reversed segment 280
3.2 The likelihood of the occurrence of the reversed segment in practical cases 281
3.3 Interpretation of the triple-valued time-distance curve 283
3.4 A special case involving a discontinuous velocity function 283
3.5 Error involved in disregarding the travel-time curve at large epicentral distances 285
3.6 Possibility of confusing curves of types II and III 286
PART IV. DISCONTINUOUS TRAVEL-TIME CURVES CAUSED BY SLOWER SPEED BEDS 287
4.1 Rearrangement of velocity function 288
4.2 Minimum thickness of slower speed horizon 289
4.3 Minimum thickness of slower bed 290
4.4 Interpretation of the travel-time curve beyond the discontinuity 291
Part V. COMMENTS REGARDING THE APPLICATION OF THE ABOVE RESULTS TO A SPHERICAL EARTH 292
5.1 Failure of previous method in the case of a slower-speed shell 293
5.2 Occurrence of the triple-valued travel-time curve 293
CONCLUSIONS 294

The theory of the interpretation of seismic travel-time curves for refracted rays in horizontal structures is treated after the manner of Herglotz-Wiechert, under the customary assumption that the ray paths obey the laws of geometrical optics. Multiple valued travel-time curves, discontinuous velocity functions, and the discontinuous travel-time curves associated with a slower speed bed receive special consideration. It appears that interpretations satisfactory from the theoretical point of view may be obtained in these cases, although, experimentally, sufficiently complete data to meet the requirements of theory may often be difficult or impossible to obtain.

IN 1907, the problem of the direct interpretation of seismic travel-time curves for a symmetrical earth was treated by Herglotz,[1] who perceived that the determination of the velocity of elastic waves in the earth's interior

[1] G. Herglotz, Phys. Zeits. **8**, 145 (1907).

could be identified with the solution of Abel's integral equation. In 1910, Bateman[2] independently solved the same problem, and by essentially the same method. Finally, in 1910, Wiechert[3] brought the subject essentially to its present state, by a contribution of a practical nature. He succeeded in reducing the integrations involved which had been very tedious, to a quite simple and elegant process.

The special nature of the problem which Herglotz wished to solve permitted him to restrict his analysis in certain respects; first, the velocity was supposed always to increase with increasing depth; second, the variation of velocity with depth was assumed to be of such a type that no ray paths intersected. While these assumptions were justifiable in Herglotz's problem, there are other cases of the same general problem for which such restrictions may not be imposed. For example, in seismic prospecting, the presence of a slow speed layer leads to violation of the first requirement, and an acceleration in the velocity-depth function may lead to the violation of the second. Again, in the recent explorations of the upper atmosphere by acoustic travel-time data, and in the study of layering in the upper fifty miles of the earth's crust by means of local earthquakes, the two conditions mentioned need not in general be satisfied. In closing his 1907 paper, Herglotz expressed his intention of examining the problem further, free from these restrictions. However, a search of the literature seems to show that little further attention has been given to the theory of the subject.

In discussing the two restrictions noted above, it will be convenient to recast the problem slightly, by assuming a flat instead of a spherical earth. For the newer applications, such as those in seismic prospecting, in the seismic studies of the upper crust, and in the acoustic study of the upper atmosphere, it is usually appropriate to neglect the curvature of the earth. Corresponding to Herglotz's assumption of spherical symmetry, the assumption of horizontal uniformity is made, so that in the present treatment the velocity is permitted to vary only with depth.

It will be convenient to outline briefly the well-known method of Herglotz-Bateman-Wiechert, in order that some of the relationships that occur may be conveniently available for subsequent reference.

Part I. Normal Type of Time-Distance Curve

1.1 Review of Herglotz-Wiechert solution

The problem treated by Herglotz may be visualized by reference to Fig. 1. The source or focus is at the ground's surface. The velocity of the elastic wave is supposed to increase with depth, as indicated by the graph in the lower left. As in the optical analogue, the energy is assumed to be propagated along the curved ray paths shown, in accordance with Fermat's principle of least time; and for the present case of a horizontally uniform medium, it is

[2] H. Bateman, Phil. Mag. **19**, 576 (1910).
[3] Wiechert and Geiger, Phys. Zeits. **11**, 294 (1910).

easily shown that Fermat's principle implies Snell's familiar law of optical refraction; that is, along any given ray the condition

$$\sin i/v = \sin i_0/v_0 \tag{1}$$

is satisfied, where v_0 is the velocity at the surface, and i_0 the initial angle of incidence, or, by symmetry, the angle of incidence at the point of emergence of the ray. The value of $\sin i_0$ as a function of epicentral distance is easily obtained from the travel-time curve. For, in Fig. 2, if S represents the surface of the wave front just before emergence, the ratio of the wave velocity

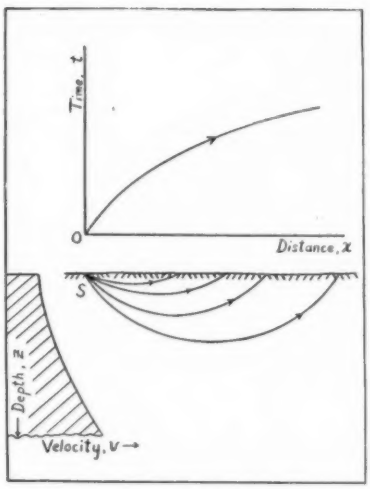

Fig. 1. Normal type of travel-time curve. Normal path.

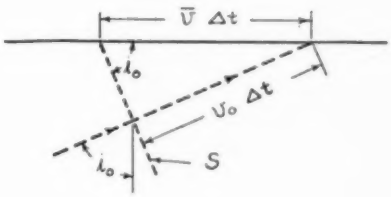

Fig. 2.

v_0 to the apparent velocity of propagation along the surface, $\bar{v}$, as read from the travel-time curve, is $\sin i_0$.

$$v_0/\bar{v} = \sin i_0. \tag{2}$$

On substituting (2) in (1) we obtain the following relation characterizing any given ray:

$$\sin i = v/\bar{v}. \tag{3}$$

Thus at the deepest point of any path, where $\sin i = 1$, the wave velocity is precisely the travel-time velocity at the point of emergence of this ray. It remains, therefore, only to determine the maximum depth, z_p, attained by a ray of travel-time velocity $\bar{v}_p$.

The horizontal distance, x, traversed along any ray from the origin to a depth z, is

$$x = \int_0^{z_1} \tan i dz$$

which, by using Eq. (3), may be written

$$x = \int_0^{z_1} \frac{dz}{\bar{v}\{1/v^2 - 1/\bar{v}^2\}^{1/2}}. \tag{4}$$

When the upper limit z_1 is taken as the deepest point of the ray, this equation may be identified with Abel's integral equation,

$$f(y) = \int_a^y u(\lambda)d\lambda/(y - \lambda)^n,\ 0 < n < 1 \tag{A}$$

whose solution is[4]

$$u(t) = \frac{\sin n\pi}{\pi} \frac{d}{dt}\int_a^t \frac{f(y)dy}{(t - y)^{1-n}}. \tag{B}$$

If we write $\Delta = 2x_m$ so that Δ is the emergence distance of the ray of apparent velocity $\bar{v}$, and introduce the substitutions

$$\rho \equiv 1/v^2;\ \xi \equiv 1/\bar{v}^2;\ f(\xi) \equiv (\Delta/2)\cdot\bar{v}, \tag{5}$$

then Eq. (4) becomes

$$f(\xi) = \int_{1/v_0^2}^{\xi} \frac{(dz/d\rho)d\rho}{(\rho - \xi)^{1/2}} \tag{6}$$

where ρ is a function of z alone, and ξ a function only of Δ. Abel's solution of (6) is:

$$\pm \frac{1}{i} \frac{dz}{d\rho} = \frac{1}{\pi} \frac{d}{d\rho}\int_{1/v_0^2}^{\rho} \frac{f(\xi)d\xi}{(\rho - \xi)^{1/2}}$$

or

$$z = \pm \frac{1}{\pi}\int_{1/v_0^2}^{\rho} \frac{f(\xi)d\xi}{(\xi - \rho)^{1/2}}, \tag{7}$$

the constant of integration being zero. The quantities which enter the integral in Eq. (7) are all known, and hence this equation is the desired relation expressing z as a function of ρ, and hence also of v. However, the numerical evaluation of the integral was tedious until Wiechert[3] pointed out the following convenient method.

Eq. (7) is rewritten in terms of the original notation of Eq. (5) above and then the velocity, v_p, corresponding to a given value of the upper limit ρ is replaced throughout by the equal apparent velocity, $\bar{v}_p$. Then, noting that $\bar{v}d(1/\bar{v})^2 = 2d(1/\bar{v})$, Eq. (7) becomes

$$z_p = \pm \frac{1}{\pi}\int_{1/v_0}^{1/\bar{v}_p} \frac{\Delta\, d(1/\bar{v})}{[(1/\bar{v})^2 - (1/\bar{v}_p)^2]^{1/2}}$$

or,

$$z_p = -\frac{1}{\pi}\int_{\cosh^{-1}\bar{v}_p/v_0}^{0} \Delta\, d[\cosh^{-1}\bar{v}_p/\bar{v}]. \tag{8}$$

[4] Maxime Bôcher, *An Introduction to the Study of Integral Equations*, Cambridge Univ. Press, 1909, p. 9.

If this is integrated by parts the integrated term vanishes, since $\Delta = 0$ when $\bar{v} = v_0$. Hence

$$z_p = (1/\pi) \int_0^{\Delta_p} \cosh^{-1} (\bar{v}_p/\bar{v}) d\Delta. \tag{9}$$

Here Δ_p is the epicentral distance for which the apparent velocity is $\bar{v}_p$. This is essentially Wiechert's well-known formula, except that his term $r_0 \log [r_0/(r_0 - z)]$ which occurs on the left-hand side in the case of a spherical earth[3] has been replaced by its limit z as r_0 approaches infinity.[5]

The integration indicated is very simply carried out graphically, after reading the required inverse hyperbolic cosines from a table. Fortunately, relatively few points usually suffice to define the $\cosh^{-1} (\bar{v}_p/v)$ curve within the needed accuracy, so that in practice the formula (9) furnishes a simple and rapid method of interpreting the travel-time curve.

1.2 Validity of the solution above

Bôcher[4] gives as the necessary and sufficient conditions that Abel's Eq. (A) above, have the continuous solution (B) in the interval $a \leqq \xi \leqq b$, the following three: (a) $f(\xi)$ must be continuous in the interval; (b) $f(a) = 0$; (c) $\int_a^x f(\xi) d\xi/(x - \xi)^{1-n}$ must have a continuous derivative in the interval. The condition (c) is fulfilled whenever (a) and (b) are true and $f(\xi)$ has a derivative which is finite with at most a finite number of discontinuities.[4] For brevity, we shall refer to these as Bôcher's conditions.[6]

[5] See also Maurice Ewing and L. Don Leet, *Geophysical Prospecting* A.I.M.E., 1932, p. 269.

[6] These conditions are, however, somewhat more severe than need be, because only continuous functions $f(\xi)$ and finite[7] functions $u(\rho)$ are contemplated. The function $f(\xi)$ may, however, possess finite discontinuities without invalidating the solution, as may be easily verified by the following example, suggested to me by Professor O. D. Kellogg. Suppose that $f(\xi)$ is discontinuous, as follows:

$$f(\xi) = 0 \quad \text{when} \quad 0 \leqq \xi < \alpha$$
$$f(\xi) = 1 \quad \text{when} \quad \alpha \leqq \xi.$$

Then, by assuming that the solution (B) holds:

$$u(\rho) = 0, \quad \text{when} \quad 0 \leqq \rho \leqq \alpha$$
$$\text{and } u(\rho) = \frac{1}{\pi} \frac{d}{d\rho} \int_\alpha^\rho \frac{d\rho}{(\rho - \xi)^{1/2}} \quad \text{when} \quad \alpha \leqq \rho.$$

If the above values for u be substituted in Eq. (A) we get the check:

$$f(\xi) = 0 \quad \text{when} \quad 0 \leqq \xi < \alpha$$
$$\text{and } f(\xi) = \frac{1}{\pi} \int_\alpha^\rho \frac{d\rho}{(\rho - \alpha)^{1/2} (\xi - \rho)^{1/2}} = 1 \quad \text{when} \quad \xi > \alpha.$$

Clearly, any prescribed function $f(\xi)$ having a definite number of finite discontinuities may be expressed as a continuous function plus discontinuous functions of the step type used above. Hence the solution for the Abelian integral equation formed for such a function $f(\xi)$ will be the sum of component solutions each obtained by the usual formula (B).

The solution of Abel's equation when the condition $f(a) = 0$ is not satisfied is given by Goursat, Acta Mathematica **XXVII**, 131 (1903).

[7] M. Bôcher, reference 4, theorem 2, p. 4.

Part II. A Transitional Case

2.1 A focus point as a discrete point

A second type of travel-time curve will receive mention despite its very special nature, because it is the transitional case between the first type mentioned, and the third type presently to be discussed. In it, all the rays are brought to a common focus, both as regards time and distance, so that the time distance curve degenerates into a single point, marked P on Fig. 3a. The velocity depth function which produces this result is easily found on writing. Eq. (4) in the form

$$x_m = \int_{v_0}^{v_m} \frac{v(dz/dv)dv}{(v_m^2 - v^2)^{1/2}} \tag{10}$$

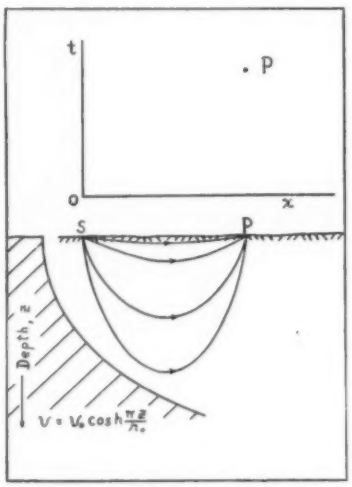

Fig. 3a. Travel-time curve a single point. Special case.

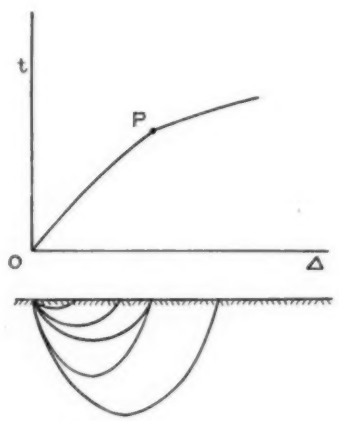

Fig. 3b. Focus point in a continuous travel-time curve.

setting $x_m = r_0/2$, a constant, $v^2 \equiv \xi$ and $v_m^2 \equiv \lambda$; and solving the resulting integral equation,

$$x_m = \tfrac{1}{2}\int_{v_0^2}^{\lambda} \frac{(dz/dv)d\xi}{(\lambda - \xi)^{1/2}} \tag{11}$$

for dz/dv. It results that

$$v = v_0 \cosh(\pi z/r_0) \tag{12}$$

is the required function which brings all rays to the common emergence distance $\Delta = r_0$.

The elapsed time, $t/2$, corresponding to the half range x_m in Eq. (10) is

$$\frac{t}{2} = \int_0^{z_m} \frac{dz}{v\cos i} = \int_{v_0}^{v_m} \frac{v_m(dz/dv)dv}{v(v_m^2 - v^2)^{1/2}} \tag{13}$$

where z_m denotes the depth to the bottom of the ray path. By using $dz/dv = (r_0/\pi)\ 1/(v^2 - v_0^2)^{1/2}$ from Eq. (12), and putting $\eta \equiv (v/v_m)^2$, Eq. (13) becomes:

$$\frac{t}{2} = \frac{r_0}{2\pi v_m} \int_{(v_0/v_m)^2}^{1} \frac{d\eta}{\eta(1-\eta)^{1/2}(\eta - (v_0/v_m)^2)^{1/2}}. \tag{14}$$

This yields, on integration,

$$\frac{t}{2} = \frac{r_0}{2\pi v_m}\left(\pi \frac{v_m}{v_0}\right) = \frac{r_0}{2v_0}.$$

Thus the times of emergence, t, are also equal for all rays, and the travel-time curve reduces to the single point, $\Delta = r_0$, $t = r_0/v_0$. The locus of such singular points is, then, the straight line $t = \Delta/v_0$.

2.2 A focus point as a point in a continuous travel-time curve

It is of interest to examine whether a focus[8] point such as this can be a point in a continuous travel-time curve through it. In Eq. (11) the half range x_m was expressed as a function of λ, say $\psi(\lambda)$, where it will be recalled $\lambda \equiv v_m^2$. (a) If $v(z)$ be assumed continuous and increasing, dz/dv in Eq. (11) will be finite, and $\psi(\lambda)$ will be continuous. (b) Furthermore, $d\psi/d\lambda$ will be continuous whenever dz/dv is a continuous function of ξ and has a finite derivative which possesses at most a finite number of discontinuities.[9] (c) By Eq. (11), $\psi(v_0^2) = 0$.

With these assumptions, then, Bôcher's three conditions on $\psi(\lambda)$ are satisfied, so that the Eq. (11), i.e.,

$$\psi(\lambda) = \tfrac{1}{2} \int_{v_0^2}^{\lambda} \frac{(dz/dv)d\xi}{(\lambda - \xi)^{1/2}} \tag{11a}$$

possesses a unique continuous solution. But none of the conditions (a), (b), or (c) above is invalidated by allowing $\psi(\lambda) \equiv x_m$ to assume arbitrary values involving continuous positive or negative values of its derivative, $d\psi/d\lambda$. In particular, we may assign to $\psi(\lambda)$ a *constant* value over a portion of the range in λ. But this condition on $\psi(\lambda)$ is the condition that there shall be a focus point. We therefore conclude that $\psi(\lambda)$ may be arbitrarily assigned subject to the conditions (a), (b), and (c) above to insure the existence of focus points at any desired epicentral distances. The requisite velocity function for establishing this result is yielded by solution of Abel's equation for dz/dv.

A travel-time curve may therefore consist of two segments meeting at a focus point. Since $v(z)$ was assumed increasing, the slope of the travel-time curve will be decreasing, and there will appear to be a *discontinuity* in slope at the focus point, as in Fig. 3b. However, in interpreting a travel-time curve of this type, it is clear that the slope must be regarded as changing continu-

[8] It will be sufficient here to consider only the focusing of the rays with respect to *distance*, because as is pointed out in paragraph 3.3, a focus in time is always implied by one in distance.

[9] M. Bôcher, reference 4, theorem 3, p. 5.

ously at the focus point through all values between the two slopes on either side of this point.

Part III. Reversed Travel-Time Curves

Whenever the half range x (in Eq. (10)) of the rays decreases locally with z, crossing of the paths will occur, as illustrated in Fig. 4. This condition produces a travel-time curve which reverses on itself as at point 1 (Fig. 4) and continues, always concave upward, from point 1 to point 2 where it may again reverse and assume the normal concave-down type. The segments meeting at the cusps at point 1 and 2 are always mutually tangent. The segment 1, 2

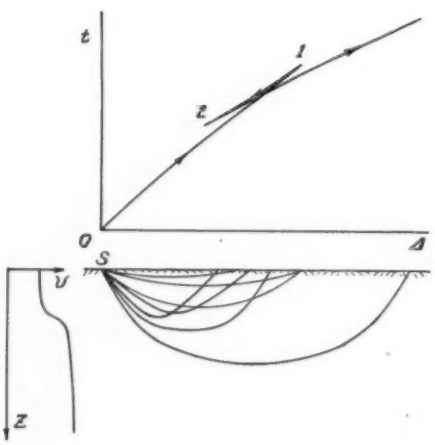

Fig. 4. Triple valued travel-time curve.

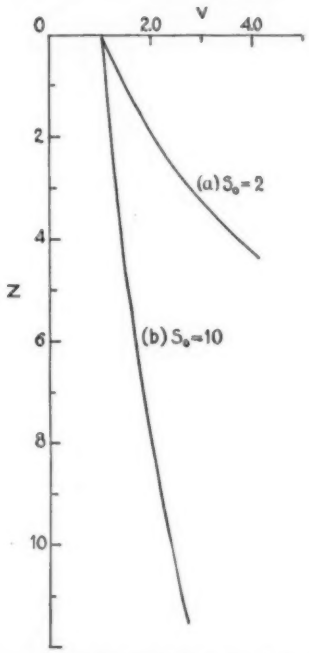

Fig. 5. Examples of velocity function which produce the triple valued curve.

will be referred to as a "reversed segment," because rays proceeding from the source at steepening angles of dip describe this segment in the direction of decreasing Δ. This type of travel-time curve has been long recognized in pure seismology,[10] but its interpretation is usually (erroneously) held to be beyond the scope of the Herglotz-Wiechert theory.[11] Its occurrence in seismic prospecting appears to be a much more common phenomenon than is generally supposed.

3.1 Condition for the occurrence of a reversed segment

The half range x traversed by a ray in attaining its vertex was expressed by Eq. (10). At the vertex, in order that the ray may turn back towards the

[10] B. Gutenberg, Handb. d. Geophysik, Borntraeger IV-I, 62 (1929).

[11] See reference 14.

surface, the velocity must obviously be increasing with depth. Hence dx/dz will have the same sign as dx/dv_m; therefore, the criterion for crossing may be taken to be $dx/dv_m<0$; and for non-crossing, $dx/dv_m>0$. This derivative is found to have the following value on differentiating Eq. (10) and then integrating by parts

$$\frac{dx}{dv_m} = v_m \left\{ \frac{(dz/dv)_0}{(v_m^2 - v_0^2)^{1/2}} + \int_{v_0}^{v_m} \frac{d^2z/dv^2}{(v_m^2 - v^2)^{1/2}} dv \right\} \equiv v_m J. \tag{15}$$

Here $(dz/dv)_0$ denotes the slope of the depth-velocity function at the surface. The condition for the existence of a reversed segment is, then, that the quantity J above be negative.[12]

(1) When the slope at the surface, $(dz/dv)_0$, is *negative*, the ray paths will be concave downwards initially, and the shallowest ray will penetrate to such a depth that the velocity at its apex is equal to the surface velocity, $v_m=v_0$. With this value for v_m, the first term in the expression for J is negatively infinite. Furthermore, if the velocity function has a curvature of constant negative sign, the integral

$$\int_{v_0}^{v_m} \frac{d^2z/dv^2}{(v_m^2 - v^2)^{1/2}} dv$$

will also be negative, and the existence of a reversed segment is assured.

(2) For positive values of the initial slope such as generally occur in the crust, the reverse segment can occur only if d^2z/dv^2 is negative over part of the range. The values which this second derivative takes near the upper limit of the integral will clearly be especially influential because of the factor $(v_m^2-v^2)^{1/2}$ occurring in the denominator.

3.2 The likelihood of the occurrence of the reversed segment in practical cases

Furthermore, it should be noted that the occurrence of a layer throughout which the velocity is nearly constant, (d^2z/dv^2 being assumed negative) is very apt to lead to crossing of the rays. For dz/dv will then be very large, and if R denotes the radius of curvature,

$$\frac{d^2z}{dv^2} = \frac{[1 + (dz/dv)^2]^{3/2}}{R} = \left(\frac{dz}{dv}\right)^3 \Big/ R$$

nearly, so the absolute value of d^2z/dv^2 will be very large under these circumstances. To illustrate quantitatively the strong tendency for the occurrence of the triple-valued type of curve the following numerical example will serve.

Example. Let the surface velocity serve as the unit for velocity, $v_0=1$. During the depth interval $0\leqq z\leqq 1$, let dz/dv be a constant, s_0, so that the velocity at unit depth is $v_1=1+1/s_0$. Thereafter, let d^2z/dv^2 be some negative

[12] This condition on the velocity function corresponds to Herglotz's condition on the travel-time curve,[1] $d^2t/d\Delta^2>0$.

constant, $-k^2$, until a depth is reached where the velocity is double that at unit depth. The postulated depth-velocity function is then, of the type

$$z = s_0(v - 1) \text{ for } 1 \leqq v < v_1$$

$$z = 1 + s_0(v - v_1) - (k^2/2)(v - v_1)^2 \text{ for } v_1 \leqq v < 2v_1.$$

Let now $-k^2$ be so determined that crossing will be initiated at the depth corresponding to $v = 2v_1$. Substituting in Eq. (15) and performing the integration, we obtain the condition

$$\frac{s_0}{[4(1 + 1/s_0)^2 - 1]^{1/2}} = k^2\left[\frac{\pi}{2} - \sin^{-1}\tfrac{1}{2}\right],$$

or

$$k^2 = \frac{0.955 s_0}{[4(1 + 1/s_0)^2 - 1]^{1/2}}.$$

Thus for (a) $s_0 = 10$ the critical value for k^2 is 4.86, and for (b) $s_0 = 2$, $k^2 = 0.676$.

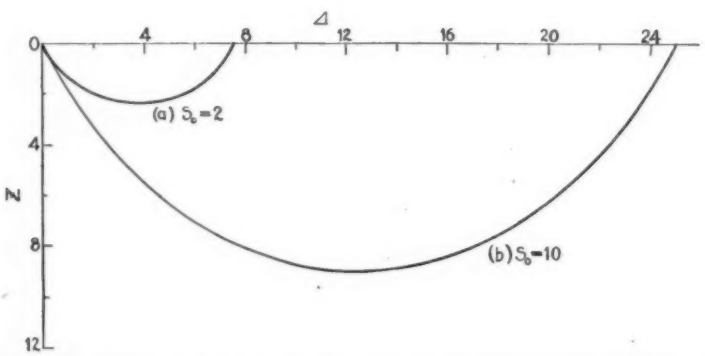

Fig. 6. Critical ray paths corresponding to the velocity functions of Fig. 5.

Larger values of k^2 in each case lead to a reversed segment in the travel-time curve. The velocity functions corresponding to these critical values are plotted in Fig. 5, and in Fig. 6 are shown the critical ray paths, which correspond. It is noteworthy that so gentle a variation in the velocity curves as is shown in Fig. 5 should be competent to produce crossing of the ray paths. *If such gradually varying functions are able to produce this result we must anticipate the frequent occurrence of the triple valued travel-time curve under conditions of seismic prospecting.*[12]

[12] The earlier computations of the heights reached by acoustic rays in the stratosphere disregarded, in effect, the triple valued nature of the travel-time curve. Thus Gutenberg (Gerland's Beitrage Z. Geophysik **27,** 22 (1930); **35,** 46 (1932) assumed a zero range in the stratosphere for grazing angles of incidence, and, in essence, a "normal" travel-time curve of type I. This oversight was pointed out by Whipple (Gerland's Beitrage Z. Geophysik **31,** 158 (1931)) who obtained somewhat higher altitudes for a given temperature on recomputing the data. Whipple's method avoids consideration of the "reversed" travel-time curve by the use of the solution of the Abelian equation in the form of Eq. (8) instead of Eq. (9).

3.3 Interpretation of the triple-valued time-distance curve

If the range, $\Delta/2$, and the time, $t/2$, to the vertex of a ray are written in the form

$$\Delta/2 = \int_0^{z_m} \tan i \, dz$$

$$t/2 = \int_0^{z_m} dz/v_m \sin i \cos i$$

then clearly

$$t = \Delta/v_m + 2\int_0^{z_m} (\cot i/v_m)dz$$

$$= \Delta/v_m + 2\int_{v_0}^{v_m} (\cot i/v_m)(dz/dv)dv$$

where for a given velocity function we may regard the last integral as a function only of v_m. Hence $\partial\Delta/\partial t = v_m$, or $\bar{v} = v_m$. Thus this relation, which was previously obtained (Eq. (3)) from simple geometrical considerations holds in general, and in particular, for the present case of the triple-valued travel-time curve. (Also since v_m is not zero, a focus point in the distance will imply a focus point in the time.) The other formulae used in section I are also valid so that the previous analysis is essentially unchanged by the occurrence of a reversed segment. However, as has been said, for increasing v_m the reversed segment is described in the direction of decreasing Δ, so that its contribution to the integral in Eq. (9) is negative.

A reversed segment, since it is associated with a velocity function increasing with depth, and is described in the negative sense, will necessarily be concave upwards. It meets its adjoining segments of the travel-time curve tangentially.

3.4 A special case involving a discontinuous velocity function

An instructive example of the interpretation of a triple-valued travel-time curve is afforded by the case of a contact between two uniform beds of different velocities. This case is very simple, and special methods for interpreting its travel-time curve are in common use. Indeed, the fact that the *general* method of Herglotz-Wiechert is applicable to such discontinuous cases or even to the case involving the reverse segment, seems to have been generally overlooked.[14] Therefore, despite the simpler special methods available, it seems worth while to consider this case from the point of view of the general theory, especially since this discontinuous case may be considered as

[14] For example, Gutenberg (Lehrbuch der Geophysik, Borntraeger, 1929, p. 250) writes "The (Wiechert) method is valid only for cases in which the velocity does not change discontinuously," and similarly in his Hand. d. Geophysik, **IV-1**, p. 42, "the method breaks down when discontinuities of the first order exist, because then the travel-time curve consists of several disconnected portions." Similarly, **V.** Conrad (Enzyklopädie d. Math. Wiss. **6**, part **1**, p. 449) writes "The Herglotz theorem is valid only when the rays . . . possess no focal surface."

a limiting one representative of a family of similar *continuous* cases which are not as a rule amenable to treatment by special devices.

The upper layer will be assumed to possess a thickness h, and a velocity V_0; the underlying material, a velocity V_1, $V_1 > V_0$. The resulting travel-time curve, shown in Fig. 7, will consist of three segments, the initial straight line (1) of slope corresponding to the velocity V_0, the "reversed segment" (2), and the straight line (3) corresponding to the velocity V_1. Theoretically, of course, the energy received along the straight segments is zero but to avoid such difficulties we may regard the example as the limiting case of one in which the velocity in the two regions is not constant, but increases infinitesimally with depth so that a finite energy is received, which vanishes as the

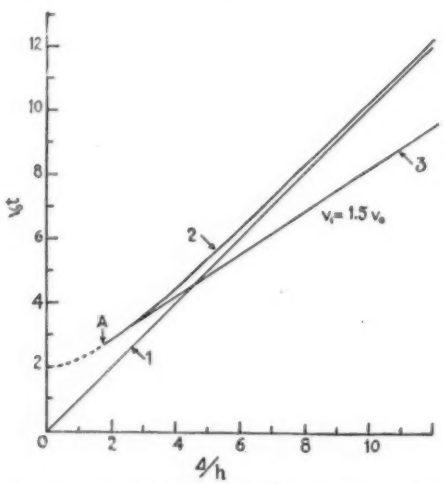

Fig. 7. Travel-time curve for the discontinuous "step" velocity function.

travel-time curve approaches the straight lines shown. The reversed segment (2) in the limit coincides with the time-distance curve yielded by the wave reflected at the surface $z = h$, and its equation is therefore:

$$t = (\Delta^2 + 4h^2)^{1/2}/v_0$$

and the apparent velocity, $d\Delta/dt$, is

$$\bar{v} = v_0(4h^2/\Delta^2 + 1)^{1/2}. \tag{15a}$$

The refracted travel-time curve begins at the point marked A, (Fig. 7) which corresponds to the angle of total reflection and therefore has coordinates:

$$\begin{cases} \Delta = 2h/[(v_1/v_0)^2 - 1]^{1/2} \\ t = (2hv_1/v_0)(v_1^2 - v_0^2)^{1/2}. \end{cases}$$

To the left of this point the curve corresponds to the reflected wave alone.

The interpretation of this travel-time curve obtained in accordance with the general method is as follows. For any point on the segment (3), velocity V_1, the corresponding depth is given by the formula (see Eq. 9)

$$\pi z = \int_0^{\infty} \cosh^{-1} \frac{v_1}{v_0}\, d\Delta - \int_{2h/[(v_1/v_0)^2-1]^{1/2}}^{\infty} \cosh^{-1} \frac{v_1}{v_0(4h^2/\Delta^2+1)^{1/2}}\, d\Delta$$

where the second integral represents the contribution of the reverse segment. On substituting $v_1/v_0 \equiv k$ and $k/(4h^2/\Delta^2+1)^{1/2} \equiv x$ this becomes

$$\pi z = \int_0^{2h/(k^2-1)^{1/2}} \cosh^{-1} k\, d\Delta + \int_1^{k} \frac{(\cosh^{-1} k - \cosh^{-1} x)}{(k^2 - x^2)^{3/2}}\, 2hk^2 dx. \quad (16)$$

After an integration by parts this yields, as it should,

$$\pi z = \pi h. \quad (17)$$

The depth corresponding to *any velocity* on the *reversed segment is also readily seen to be h*. For at any point P on this segment, of epicentral distance Δ_p and apparent velocity v_p, the depth z_p is given as before by

$$\pi z_p = \int_0^{\Delta_p} \cosh^{-1} \frac{v_p}{v_0}\, d\Delta + \int_{\Delta_p}^{\infty} \left\{ \cosh^{-1} \frac{v_p}{v_0} - \cosh^{-1} \frac{v_p}{v_0(4h^2/\Delta^2+1)^{1/2}} \right\} d\Delta.$$

Put

$$v_p/v_0 \equiv k', \text{ and } x \equiv k'/(4k^2/\Delta^2+1)^{1/2}.$$

Now by (Eq. 15a)

$$v = v_0(4h^2/\Delta^2+1)^{1/2}$$

$$\Delta = 2hv_0/(v^2 - v_0^2)^{1/2}.$$

Hence

$$\Delta_p = 2h/(k'^2-1)^{1/2}.$$

Also $\Delta = \Delta_p$ implies

$$x = k'(4h^2/\Delta_p^2+1)^{1/2} = 1$$

and $\Delta = \infty$ implies

$$x = k'.$$

Thus

$$\pi z_p = \int_0^{2h/(k'^2-1)^{1/2}} \cosh^{-1} k'\, d\Delta + \int_1^{k'} \frac{(\cosh^{-1} k' - \cosh^{-1} x)2hk'^2}{(k'^2 - x^2)^{3/2}}\, dx.$$

This is precisely Eq. (16) above except that k' replaces k, and the integration obviously yields the former result $\pi z_p = \pi h$, for all points P. Thus the depth interpretation for all points along the segments (3) and (2) is uniformly h.

In summary, the interpretation yielded by this travel-time curve is the velocity function shown in Fig. 8. The depth h is yielded by the interpretation above, and the dotted portions follow from the fact that the straightness of segments (1) and (3) indicate the constancy of the velocity in the two regions involved.

3.5 Error involved in disregarding the travel-time curve at large epicentral distances

For the discontinuous depth-velocity function of this example, the segments (1) and (2) are asymptotic at infinity, and for functions of similar type, though not strictly discontinuous, the junction point of the segments

will usually occur at epicentral distances too large to be exhibited by the field data. The error involved in disregarding the contribution of these segments at large epicentral distances is seen as follows. If Eq. (17) is written:

$$\pi z = \pi h_1 + C$$

where h_1 is the depth computed when the portions of the travel-time curve at epicentral distances greater than nh are omitted and C is the correction thereby involved, then from Eq. (16)

$$C = \int_{k/[(4/n^2+1)^{1/2}]}^{k} (\cosh^{-1} k - \cosh^{-1} x)\frac{2hk^2dx}{(k^2 - x^2)^{3/2}}$$

$$= -\left(\cosh^{-1} k - \cosh^{-1}\frac{k}{[(2/n)^2 + 1]^{1/2}}\right)nh$$

$$+h\int_{k^2/[(4/n^2+1]}^{k^2} \frac{d\xi}{(k^2 - \xi)^{1/2}(\xi - 1)^{1/2}}$$

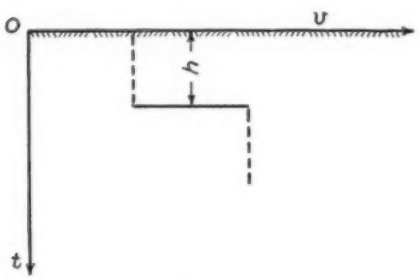

Fig. 8.

where the substitution $\xi \equiv x^2$ has been introduced in the last integral. Hence

$$C = h\left[\pi - 2\tan^{-1}(n/2k)(k^2 - 1 - 4/n^2)^{1/2}\right.$$

$$\left. - n\left(\cosh^{-1} k - \cosh^{-1}\frac{k}{(4/n^2 + 1)^{1/2}}\right)\right]. \qquad (18)$$

From this formula the value of the relative error in the depth determination for the special case $k = 1.5$ plotted in Fig. 7, and for several values of n, is as follows:

n	5	10	50
$(h - h_1)/h$	0.165	0.082	0.014

Thus the error committed in neglecting the portion of the travel-time curve at distances in excess of ten times the thickness of the upper layer is small.

3.6 Possibility of confusing curves of types II and III

The rational interpretation of travel-time curves of type III may sometimes be quite impossible in practice, due to the difficulty in identifying the reversed segment (2) and in constructing a correct travel-time curve from

the field data. The construction of the reversed segment involves the recognition of *third* arrivals of the wave pulses, but when the *second* arrivals corresponding to the extension of the (nearly) straight portions (1) and (3) of the travel-time curves can be recognized, the existence of the connecting segment (2) is thereby established. It should then often be possible to establish the general form of the connecting segment with sufficient accuracy by the conditions that it must be concave upward and must meet the two known segments tangentially.

In any event, it is of theoretical importance to distinguish between a travel-time curve having a discontinuity in slope at a focus point, as in Fig. 3b, and one which has a reversed segment, as in Fig. 4, for the latter type of curve implies a much more rapidly increasing velocity with depth than the former. To illustrate this point suppose the later arrivals in the travel-time curve of Fig. 7 to be disregarded, so that the curve consists only of the (nearly) straight segments (1) and (3) up to their point of intersection. By the standard formula, the interpretation of this curve is

$$z = (\Delta_i/\pi) \cosh^{-1} v/v_1$$

or

$$v = v_1 \cosh \pi z/\Delta_i$$

where Δ_i is the abscissa of the point of intersection, and is therefore equal to $2h\left[(v_2/v_1-1)/(v_2/v_1+1)\right]^{1/2}$, where h is the depth yielded by the solution of the complete travel-time curve of Fig. 7. As mentioned in §2.2, at the point of intersection the apparent velocity must be assumed to change continuously from its upper value v_2 to its lower one, v_1.

This interpretation, a hyperbolic cosine velocity-function, is quite different from the step function yielded by the complete curve. Indeed, when $v_2=1.5\ v_1$, as in the example of Fig. 7, the hyperbolic cosine formula yields $z=3.04h$, instead of $z=h$ as previously obtained for the case of the complete curve, as the depth for which the velocity reaches the value v_2. This factor of 3 to 1 is especially noteworthy because the two travel-time curves considered are identical as to first arrivals, and the subsequent arrivals may easily escape notice on the record. The possibility of confusing these two types of curves and of obtaining mistaken interpretations is apparent.

Part IV. Discontinuous Travel-Time Curves Caused by Slower Speed Beds

A fourth type of time-distance curve is the discontinuous one which occurs when a slower speed bed is present. In this case, as illustrated by Fig. 9, the ray which enters the slower bed at grazing incidence is deflected downwards and does not reverse until it has penetrated to such a depth that the velocity has again attained its previous maximum. This ray may emerge at an epicentral distance considerably beyond that of its neighbor, so that a dead zone in which no energy is received results at the surface. In such cases, as is well known, it is impossible to deduce from the travel-time curve unique values for the seismic velocities at depth. Nevertheless, the theory of this

type of curve supplies us with extremal solutions which may permit deductions of satisfactory geological accuracy. In considering the theory of this case, the travel-time curve is as usual assumed to be completely known from the field data. The required degree of completeness in the definition of travel-time curves containing a gap is, however, by no means assurable from the experimental point of view. This difficulty, however, is properly disregarded in considering the narrower question of the theoretical possibilities in interpreting the ideal travel-time curves themselves.

4.1 Rearrangement of the velocity function

In dealing with the slower speed bed, it is convenient to utilize the following fact. The portion of a travel-time curve which is generated by rays which have penetrated below any reference level, z_1, is unaffected by any

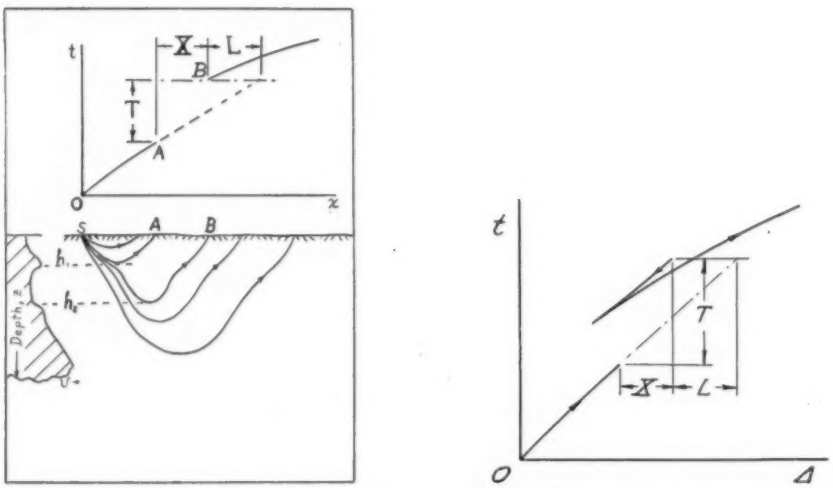

Fig. 9a. and Fig. 9b. Discontinuous travel-time curve corresponding to slow speed bed.

rearrangement or "shuffling" of the velocity function in the region above this level. This is perhaps obvious, but may be made clear as follows. The range x of any ray at its intersection with the level of reference z_1, is expressible by the integral:

$$x = \int_0^{z_1} \tan i \, dz.$$

Here, tan i at any level is fixed along any ray only by the velocity at that level, through Snell's law. Thus any rearrangement of the velocity function determines a corresponding rearrangement of the values of tan i and the area denoted by the integral remains unchanged by the process. Also, the angle of emergence just below the level z_1 is fixed for any ray by the velocity at this level. Hence for all such rays the initial conditions, i.e., the angle of incidence and the x coordinate, just below the level of reference are unaltered by any vertical rearrangement of the velocities above this level. Conse-

quently the geometry of the subsequent portions of the ray paths remains unchanged, as does the corresponding part of the travel-time curve.

4.2 Minimum thickness of slower speed horizon

In general, the velocity will have arbitrary variations in the slow speed bed, subject of course to the restrictions that $v < V$ where V is the previously attained maximum. But in accordance with the previous paragraph we may imagine the velocities in the slower speed bed rearranged to give a non-decreasing function, without altering the observed travel-time curve in any way. At the boundaries of the gap in the travel-time curve, the apparent velocities will be V, the seismic velocity at the boundaries of the slower bed. The velocity function in this bed is subject to the restriction that it yield the observed gap in the travel-time curve, which, let us say, has a discontinuity T in the time, and X in the distance. The two conditions imposed are, then

$$T/2 = \int_{z_1}^{z_2} dz/v \cos i \tag{19}$$

$$X/2 = \int_{z_1}^{z_2} \tan i \, dz \tag{20}$$

where z_1 is the known depth to the top of the bed as deduced by interpreting the initial part of the travel-time curve to the left of the gap, and z_2 is unknown. From these equations we may fix an upper possible limit for z_2, as follows: Eq. (19) may be written:

$$\frac{T}{2} = \int_{z_1}^{z_2} \frac{(\tan i + \cot i)}{V} dz = \frac{X}{2V} + \int_{z_1}^{z_2} \frac{\cot i}{V} dz. \tag{21}$$

Instead of considering T fixed and z_2 unknown, let us consider for the moment z_2 to be constant, and seek the velocity function which minimizes T for fixed X. The above equation may be written:

$$\frac{T}{2} = \frac{X}{2V} + \int_{v_1}^{V} \frac{[1 - (v/V)^2]^{1/2}}{v} \frac{dz}{dv} dv.$$

Euler's test[15] then provides the condition for a minimum

$$[1 - (v/V)^2]^{1/2}/v = \text{constant} = (1/V) \cot i.$$

Hence for any value of X the minimizing ray path is a straight line, i = constant. In view of the auxiliary condition (Eq. (20)) the necessary value for i is:

$$i = \tan^{-1} X/2(z_2 - z_1).$$

If h is the thickness of the bed, the minimum time, T_m, is then, from Eq. (21)

$$\begin{aligned} T_m/2 &= (h/V)\{\tan i + \cot i\} \\ &= (X/2V)[1 + 4h^2/X^2]. \end{aligned} \tag{22}$$

[15] A. R. Forsyth, *Calculus of Variations*, Cambridge Univ. Press, 1927, p. 16.

Thus for fixed X, T_m and h increase or decrease together. Hence for a given discontinuity T, the maximum thickness h is, as given by Eq. (22):

$$h = \left[\frac{VX}{2}\left(\frac{T_m}{2} - \frac{X}{2V}\right)\right]^{1/2} = \tfrac{1}{2}(XL)^{1/2} \tag{23}$$

where L denotes $VT - X$, and is the distance marked in Fig. 9.

It follows that the velocity v_u, which insures the maximum thickness for the slower layer has the constant value

$$v_u = V \sin i = V \frac{X/2}{(XL/4 + X^2/4)^{1/2}} = \left(\frac{VX}{T}\right)^{1/2}. \tag{24}$$

4.3 Minimum thickness of slower bed

The minimum thickness of a slower horizon consistent with observed discontinuities at the gap in the travel-time curve is also easily found. In any actual problem, one may always fix a limiting value, v_l, below which the velocity surely will not fall in any beds which can be present. This minimum velocity will evidently give a minimum thickness for the slower bed. However, in order to satisfy the observed discontinuity, X, in the epicentral distance, an infinitesimal thickness must be considered added to the lower part of the slow layer, in which the velocity increases very rapidly from the value v_l to its value V at the termination of the slower bed. The ray path will then be as illustrated in Fig. 10, from which the discontinuity T is found to be:

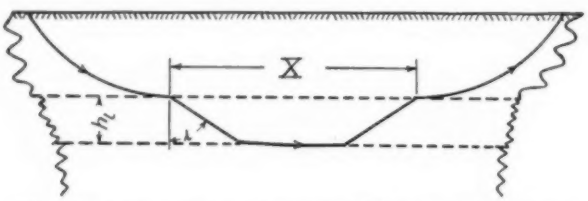

Fig. 10. Ray path for minimum thickness of slower bed.

$$\frac{T}{2} = \frac{2h_l}{V \sin 2i} - \frac{X/2 - h_l \tan i}{V}.$$

Hence the minimum thickness, h_l, is

$$h_l = \frac{\tan i}{2}\{TV - X\} = \frac{L}{2}\frac{v_l}{(V^2 - v_l^2)^{1/2}}.$$

We have determined, then, the maximum and minimum thickness for the slower speed layer, and the values of the velocities which correspond. By using these results, interpretations for the remaining travel-time curve beyond the gap may be obtained.

4.4 Interpretation of the travel-time curve beyond the discontinuity

After interpreting the initial part of the travel-time curve up to the gap in the standard way, we may use this result to form two auxiliary depth-velocity functions. (1) The first function is a combination of this result with the solution corresponding to the maximum thickness of the slower speed bed, but rearranged or "shuffled" to give a non-decreasing function. (2) The second is the similar non-decreasing rearrangement formed for the minimum thickness and velocity of the slower bed.

As has been said, the travel-time curve beyond the gap commences with a slope to correspond with the boundary velocity of the slower bed, V. Beyond this, however, we may not in general say what its subsequent form or type will be, but for simplicity we will assume that no additional slower beds occur at depth, so that the subsequent travel-time curve will at all events correspond to velocities increasing in depth.

We have, then, to consider the two known, but artificial, velocity functions (1) and (2) which are constructed as explained for the slower bed and the region above it; and the known second segment[16] of the travel-time curve which refers to the region below the gap.

From the known upper velocity functions (1) and (2) the corresponding travel-time curves may be computed. These curves will necessarily contain a "reversed" segment, asymptotic to a straight-line segment extending to infinity (as illustrated in section III) by virtue of the layer of *constant* velocity which enters the velocity-functions. In each case, of course, these travel-time curves will join the second segment of the original curve continuously for this condition was imposed in satisfying the discontinuities at the gap. On combining these curves, we obtain two continuous travel-time curves of the form shown in Fig. 11, of which the segments marked (2) are alike. These curves are now interpretable by the usual graphical method, and yield two extremal interpretations for the region below the slower bed, one corresponding to the assumption of maximum thickness, the other to the assumption of minimum thickness for it.

Thus our complete interpretation of the discontinuous travel-time curve involves three parts; (1) the interpretation gained from the initial segment in the normal way; (2) a maximum and minimum interpretation gained from the gap, and (3) the corresponding two interpretations gained from the second segment as described above. The result is two velocity functions such as are sketched in Fig. 12. In practical cases it will probably often be found that

[16] This second segment, let is be noted, may be of a complex form, as produced, let us say, by a combination of segments of the normal and reversed type. (However, the occurrence no additional gaps or discontinuities has been postulated.) The possibilities regarding the form of this second part are in no way limited by the character of the known functions (1) and (2) as deduced for the region above the bottom of the slower bed. For in cases of velocities increasing with depth, as noted in paragraph 2.2, the derivative $d\psi(\lambda)/d\lambda$ may be considered to vary at will from negative to positive values, and *vice-versa*, corresponding to crossing or non-crossing of the rays. Thus in such cases the type of travel-time curve traced by rays penetrating *below* a given level is essentially unrestricted by the velocity function *above* this level.

these two solutions are sufficiently alike so that their mean may be used without danger of an error significant from the geological point of view.

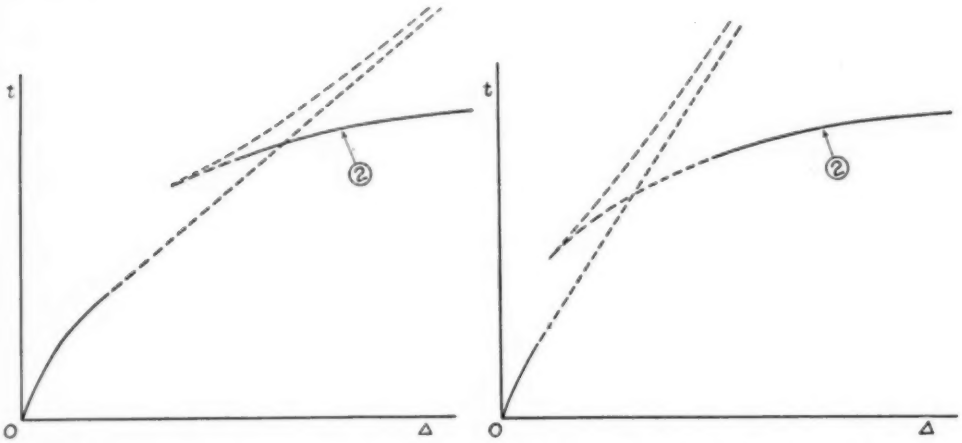

Fig. 11. Auxiliary travel-time curves for interpretation of region below slower bed.

In case an additional slow speed bed is encountered at depth, the above procedure of course leads to four, instead of two, tentative solutions, etc.

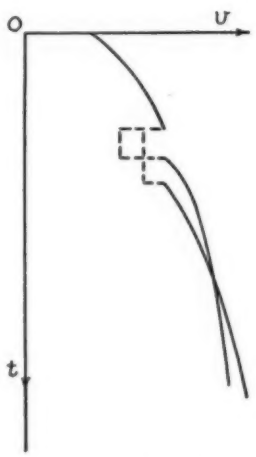

Fig. 12. Extremal interpretations for case of slower bed.

Part V. Comments Regarding the Application of the Above Results to a Spherical Earth

With slight modifications the above discussion of seismic travel-time curves for a flat earth will in general also apply to the corresponding topics in the case of a spherically symmetrical earth. But an exception to the rule, and one modification of the foregoing results will be specifically mentioned.

5.1 Failure of the previous method in the case of a slower speed shell

The analogous interpretations of the region inside a slower speed shell in a spherical earth may not be obtained by the method used in the case of a flat earth, i.e., by the device of rearranging the velocity function in a non-decreasing way. For in the spherical case the travel-time curve corresponding to the underlying region *is* altered by applying such a process to the region above. More specifically, the angular range traversed by a ray in passing between the levels r_1 and r_2 is

$$\theta = -\int_{r_1}^{r_2} \tan i dr/r$$

where $\tan i$ is given by the well-known relation, $r \sin i/v = r_0 \sin i_0/v_0 =$ constant along any ray. Here r_0 is the radius of the earth, r the radial distance from its center, and the other symbols are as previously defined. Thus the expression for θ is of the form

$$\theta = -\int_{r_1}^{r_2} f(r, r/v)dr$$

$$= \int_{r_1}^{r_2} f(r, \phi(r))dr.$$

In general this is obviously not constant when $\phi(r)$ is varied by the device of "shuffling" $v(r)$; hence the former method fails in this case.

5.2 Occurrence of the triple valued travel-time curve

The criterion for the crossing of ray paths in a spherical earth which corresponds to Eq. (16) above may be obtained as before by writing the half range to the bottom of a ray as an integral in the variable v, and differentiating with respect to the upper limit. Thus

$$\frac{\Delta m}{2r_0} = -\int_{r_0}^{r_m} \frac{\tan i dr}{r}$$

$$= -\int_{r_0}^{r_m} \frac{(r_m/v_m)(dr/r)}{[(r/v)^2 - (r_m/v_m)^2]^{1/2}}$$

$$= -\int_{v_0}^{v_m} \frac{v(dr/dv)dv}{[(v_m r/r_m)^2 - v^2]^{1/2}}$$

and

$$-\frac{1}{2r_0}\frac{d\Delta_m}{dv_m} = \frac{v_m r_0}{r_m^2}\left[\frac{(dr/dv)_{r=r_0}}{[(r_0 v_m/r_m)^2 - v_0^2]^{\frac{1}{2}}} + \int_{v_0}^{v_m} \frac{(d^2r/dv^2)dv}{[(r_0 v_m/r_m)^2 - v^2]^{1/2}}\right].$$

Thus the condition for the occurrence of the triple valued time-distance curve is:

$$\frac{(dr/dv)_{r=r_0}}{[(r_0 v_m/r_m)^2 - v_0^2]^{1/2}} + \int_{v_0}^{v_m} \frac{(d^2r/dv^2)dv}{[(r_0 v_m/r_m)^2 - v^2]^{1/2}} > 0 \qquad (25)$$

and *vice-versa*.

The application of this criterion to a velocity function which approximates that for the earth seems to indicate that there is a much lesser likelihood for the occurrence of a triple valued curve than was noted above in the case of seismic prospecting. For example, let the seismic velocity function in the earth be taken to be that given by Gutenberg.[17] Between the surface and a depth of 1200 km a linear variation, $v = 32.7 - 24\, r/r_0$ prevails, corresponding to a velocity of 7.9 km/sec. at 60 km depth and 12.2 km/sec. at 1200 km depth.

Now consider a slightly different function commencing with the same initial velocity, having a constant slope 10 percent less than the above until the depth corresponding to $v = 10$ is attained, and thereafter possessing a constant second derivative d^2r/dv^2 until the velocity $v = 12$ is attained. Furthermore, let the value of $d^2r/dv^2 \equiv k^2$ be so chosen that the "reversed" travel-time curve is incipient when $v = 12$. The postulated velocity function is, then

$$v = 29.3 - 21.6r/r_0 \text{ when } v < 10$$

and,

$$r/r_0 = 0.892 - (v - v_1)/21.6 + (k^2/2r_0)(v - v_1)^2 \qquad (26)$$

when $v > v_1$. Here v_1 is taken as 10. From Eq. (25), the condition on k^2/r_0 is,

$$0 = -\frac{1}{21.6\left[(12r_0/r_m)^2 - (7.67)^2\right]^{1/2}} + \frac{k^2}{r_0}\left[\sin^{-1}\frac{r_m}{r_0} - \sin^{-1}\frac{10}{12}\frac{r_m}{r_0}\right]$$

where r_0 and k^2/r_0 also satisfy Eq. (26) formed for $v = v_m$. By trial, the solution of these equations is found to be $k^2/r_0 = 0.0175$. The resulting velocity function is

r/r_0	1.0	0.893	0.855	0.835	0.833
v	7.67	10	11	12	13

This is plotted in Fig. 13 in comparison with Gutenberg's function. There is also shown a third function which is obtained as just described, with the difference that the junction of the straight and curved portions is supposed to occur at $v = 9$ instead of $v = 10$. In both cases, the condition is imposed that incipient crossing occurs for rays which bottom at the depth where $v = 12$.

These altered velocity functions differ sufficiently from the actual one as given by Gutenberg so that it is unlikely that this requisite difference can really exist. The conclusion thus seems justified that in general the travel-time curves will not be triple valued from such a cause, or if so, at least not to such an extent as to affect significantly their interpretation at depth. This of course is in agreement with the experimental evidence and the usual conclusions relative to this point.

Conclusions

It appears that the interpretation of seismic travel-time curves in horizontal structures has a satisfactory theoretical basis, under the assumptions

[17] B. Gutenberg, *Der Aufbau der Erde*, 1925, p. 31.

made. The classical method of Herglotz-Wiechert may be extended to the general case, involving multiple valued travel-time curves, discontinuities in the velocity depth function, and also, in a certain sense, to cases involving slower speed beds. The experimental definition of the travel-time data is not, however, always sufficiently complete to fulfill the needs of the theory. The case of the slower speed bed, and some cases in which an accelerated increase of the velocity occurs with increasing depth, offer experimental difficulties in

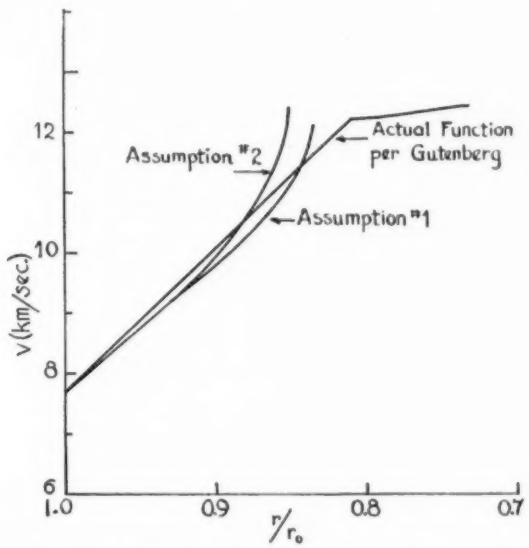

Fig. 13. Example showing velocity functions which produce triple valued travel-time curves in case of a spherical earth.

the complete identification of the travel-time curve. The errors introduced by deficiencies in the experimental data will in certain instances cause the velocity to appear to vary more gradually than is really the case.

The writer wishes to express his appreciation of the kindness of Professor P. Franklin in reading the manuscript.

The Measurement of the Phase Angles of Shielded Resistors

By LEO J. BERBERICH*
Electrical Engineering Department, Johns Hopkins, Baltimore, Md.

(Received October 3, 1932)

In this paper is discussed the problem of measurement of the small, but not always negligible, phase angles of resistors, with special reference to shielded resistors of 1000 ohms and above. Several types of shielded resistors are described briefly, among which is the ideally shielded, low-phase-angle resistor, recently constructed by the writer. The substitution method developed is one in which the resistor, the phase angle of which is desired, is compared, by means of bridge circuit, to a reference standard of a simple geometric configuration and of approximately the same resistance as that of the resistor. The results of measurements, at frequencies of 500 and 60 cycles, on three ideally shielded resistors are given. By a series connection of resistors it is possible to extend the range of the method to 50,000 ohms.

1. INTRODUCTION

AS OUR standards of accuracy progress precision of measurement becomes increasingly more important. In precise alternating current measurements cases often arise where the small phase angles of resistances cannot be neglected. Because of the generally conceded difficulty of the measurement of such phase angles only meager information appears in the literature concerning this problem. Noteworthy is the work of Grover and Curtis[1] of the Bureau of Standards, and as a general treatment of the subject it may be considered monumental. Of the early work done in this connection that of E. Giebe[2] and that of Wien and Prerauer[3] deserve consideration. In both the former and the latter a modification of Maxwell's method for the comparison of two small inductances was used. Most of the work done in this field up to the present time was carried out at frequencies in the audible range and only very little at frequencies as low as 60 cycles per second.

The question of choosing a method for this type of measurement is not settled by taking into account merely the magnitudes of the residual inductance and capacitance. The value of the resistance with which they are associated must also be considered. Thus the "time constant," which is the ratio of the "effective inductance" (resultant effect of residual capacitance and inductance) to the resistance, is a determining factor as well as the magnitude of the resistance. The problem of measuring the phase angle of a low resistance having a given time constant is, in general, different from that of a high resistance having the same time constant. In low resistance coils, 1 to

* Researsh and Development Department Vacuun Oil Company, Inc., Paulsboro, N. J.

[1] F. W. Grover and H. L. Curtis, *The Measurement of the Inductance of Resistance Coils*, Bull. Bur. Stds. **8**, 463 (1913).

[2] E. Giebe, *Prazisionsmessungen an Selbsinduktionsnormalen*, Zeits. f. Inst. **31**, 6–20, 33–52 (1911). Also see B. Hague, *A. C. Bridge Methods*, 2nd Edition, p. 216.

[3] O. Prerauer, Ann. d. Physik **53**, 772–774 (1894).

10 ohms, the magnetic field close to the wires is not entirely eliminated and gives rise to a small residual inductance. There is also, however, an electrostatic capacitance between adjacent turns and adjacent layers which tends to neutralize the inductive effect of the magnetic field. In 100 ohm coils, bifilarly wound, it has been found for low frequencies that these two effects approximately balance each other, and thus they are essentially nonreactive. When we come to resistance of 1000 ohms or above, however, we find that the effect of electrostatic capacitance predominates. If we consider this distributed shunt capacitance as lumped and connected across the terminals of the resistance, it is a simple matter to show that the capacitance effect is proportional to the product of the square of the resistance R, and the capacitance C which shunts R. Hence, the effect of capacitance increases as the square of the resistance and the higher resistances can be expected to be capacitative rather than inductive.

Grover and Curtis divided their investigation of this problem into two parts; the first part treats methods for measurement of low resistance coils, and the second part, methods adapted to coils of resistances greater than a 1000 ohms. The reason for this division is quite logical. In measurements on low resistance coils the inductance of the leads and all mutual inductance effects must be considered or else shown to be negligible. For coils of high resistance the inductance effects become negligible, and the capacitance effects between the various parts of the measuring circuit and to earth become important. The two cases thus differ essentially in that the first involves the measurement of an extremely small inductance and the second, that of an extremely small capacitance. In this paper, however, only the second case will be treated since we are here concerned mainly with shielded resistances of 1000 ohms and upward. One of the methods used by Grover and Curtis is modified by introducing certain novel features and simplifications.

In order to simplify subsequent computations the residual capacitance will be regarded as a negative inductance insofar as its effect on the phase angle is concerned. It is easy to show that the tangent of the phase angle of a coil of resistance R, inductance L, and shunt capacitance C is approximately the ratio of $2\pi f\,(L-CR^2)$ to R. Now it is convenient to call $(L-CR^2)$ the effective inductance, L', of the coil. L' will be either positive or negative according as the effect of inductance or capacitance predominates. Hence, the effective inductance may be defined as, the inductance which when multiplied by $2\pi f$ and divided by R gives the tangent of the observed phase angle. The phase angle is positive when L' is positive and negative when L' is negative.

2. Several Types of Shielded Resistors

In general every resistance contains three parasitic properties; namely, self-inductance, self-capacitance (capacitance between the various parts of the coil), and earth capacitance. Of these three, the last named is the most troublesome. The first two can be made small by the proper choice of a winding for the particular coil under consideration.[4] It is, however, not quite such a simple matter to reduce the effect of earth capacitances. Such capacitances

will cause the phase angle to vary with the position of the coil with respect to earth and also with the potential of nearby objects in the laboratory. The only remedial measure which is at our disposal is to completely shield the coil in a metal case maintained at a definite potential. This may be done in a number of ways.

The simplest method of shielding is illustrated in Fig. 1A. Here the resistance is completely surrounded by a metal container which is connected to one end of the resistance in order to fix its potential. This, however, has the effect of increasing the phase angle because of the close proximity of the shield to the resistance. The distributed capacitances from the resistance to the shield are in general greater than similar capacitances to earth would be without the shielding. But such a shield will fix the phase angle and once it is measured it can be allowed for in the computations.

As the resistance within the shield increases the effective inductance rises rapidly, approximately as the square of the resistance. The effective induc-

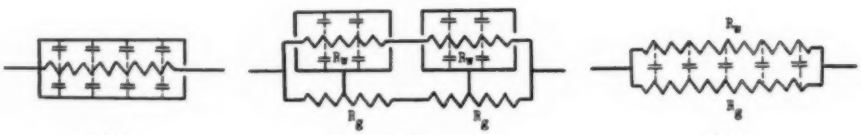

(A) (B) (C)

Fig. 1. Three types of shielding.

tance can be decreased markedly by subdividing the resistance into sections and surrounding each section with a shield. Fig. 1B shows the "working resistance," R_w, divided into two sections. The shields are maintained at a definite potential by connecting them to an auxiliary circuit R_g. This auxiliary circuit is known as the "guard circuit." Shielded resistors of this type have been described and mathematically analyzed by Orlich,[5] Kouwenhoven,[6] Hiecke[7] and Silsbee.[8] The mathematical analysis of a series connection of a number of these resistors shows that the following conditions must be fulfilled in order to obtain a minimum phase angle for the combination: (1) the potential of the shield of every unit except the first and the last must be equal to that of the midpoint of the resistance within it, (2) the potential of the shield of the first unit (low-voltage end) must be below the potential of the midpoint of the resistance within it by an amount equal to one-twelfth the voltage across the terminals of this unit, and (3) the potential of the shield of the last unit (high-voltage end) must be above the potential of the midpoint of the resistance within it by an amount also equal to one-twelfth of

[4] H. L. Curtis and F. W. Grover, *Resistance Coils for Alternating Current Work*, Bull. Bur. Stds. **8**, 495 (1913).

[5] E. Orlich and H. Schultze, Archiv. f. Elek. **1**, 1 (1912).

[6] W. B. Kouwenhoven, Washington University Studies **1**, part 1, No. 2, p. 143 (1914).

[7] R. Hiecke, Electrotech. u. Masch. **33**, 505 (1915).

[8] F. B. Silsbee, *A Shielded Resistor for Voltage Transformer Testing*, Bur. Stds. Sci. Paper No. 516, (1925).

the voltage across the terminals of this unit. In order to be able to interchange the various units of the combination or to tap off a portion of the total resistance it is often convenient not to fulfill conditions (2) and (3) and to adjust the potential of every shield equal to that of the midpoint of the resistance within it. This is done in the case of the shielded resistor in use at the Bureau of Standards.[8] The result is a slightly higher phase angle than is the case when all the conditions are fulfilled. Thus, if the circuit is so constructed that R_g is equal to R_w for every unit and the shield of every unit connected to the midpoint of R_g, we have the second case. It is obvious that when this is done the capacitance currents from R_w to the shielding are balanced; that is, just as much current will flow away from R_w to the shield in one-half of the unit as will flow back to R_w in the other half. There will be no loss of current, theoretically at least, from R_w to R_g. This type of shielding results in a marked reduction in phase angle, yet it is not negligible and in many cases must be measured.

If we carry the subdivision of the resistor to the limit where each element of the resistance R_w is shielded by a corresponding element of R_g we have what is known as the ideal type of shielding. Fig. 1C indicates schematically such a resistor. The guard circuit should be constructed so as to be coaxial with, and completely surround the working circuit. Also, the resistance must be uniformly distributed and the same for both circuits. When this is the case, even though the distributed capacitances between R_w and R_g exist, there will be no voltage across them because the potential is the same along corresponding points of the two circuits. A special case, one end grounded, of this ideally shielded resistor has been mathematically analyzed by Silsbee[8] who showed the phase angle to be extremely small, though not zero, because of the distributed earth capacitances from the guard circuit to ground. A number of such ideally shielded resistors have been actually constructed by the writer and will be described in a later paper.[9] The ultimate aim in the development of the method to be described was to obtain a measurement at 60 cycles of the extremely low values of effective inductance which one may expect with this type of shielding. The results of a series of measurements on a 10,000 ohm unit, 5000 ohm unit, and 1000 ohm unit will be given in this paper.

3. General Principles

Practically any method used to measure the effective inductance of resistance coils resolves itself into a substitution method. This affords the simplest method of eliminating the effect of parasitic influences in the circuit. Other methods have been used with some degree of satisfaction, but in the writer's opinion the substitution method is perhaps the easiest to use, does not require any very special apparatus, and gives the most accurate results. By a substitution method is meant one in which a reference standard of calculable residuals and of approximately the same resistance as the unknown is inserted in one arm of a bridge network and a balance obtained; then the

[9] W. B. Kouwenhoven and Leo J. Berberich, "*A Standard of Low Power Factor.*" To be presented at Winter Convention of A.I.E.E., New York, N. Y., (1933).

standard is replaced by the unknown and the network again adjusted to a balance by varying one arm only, all other arms being kept fixed during the substitution process. The amount of the change required in this one arm is usually so small, provided the resistance of the standard is adjusted to very nearly that of the unknown, that the change in the parasitic influences in the arm is negligible. The parasitic admittances of the fixed arms are automatically eliminated since they enter into the computations only as ratios.

Standards of reference

The standards used in this work were constructed in the form of two parallel wires of high resistance material. For 5000 ohm and 10,000 ohm standards special Nichrome wire was used, having a diameter of approximately 1.4 mils (0.035 mm) and having a resistance of approximately 250 ohms per foot. The spacing of the wires was maintained by means of four small brass pins embedded in two hard rubber spacing blocks, the latter serving as supports at the ends of the standard. The two parallel wires were joined at the far end and the open end was placed near the bridge circuit. At the open end, the standard was fitted with short copper leads which dipped into mercury wells placed as closely as possible to the brass pins in the spacing block. The leads from the bridge circuit made contact with two other mercury wells, one beside each of the two for the standard. This permitted the insertion of the standard in the bridge by merely dropping two small copper links, one each into the two pairs of wells. The two spacing blocks were placed at such a distance that the wires were supported without appreciable sagging. The 10,000 ohm standards were approximately 20 feet long. In order to obtain a standard of more than a few feet in length for the 1000 ohm case, No. 40 A.W.G. manganin wire was used instead of the high resistance Nichrome. It is necessary that the standard have a considerable length in order to make the end effects negligible.

Computation of residuals for standards

The residuals of a standard such as described above can be easily computed. The inductance due to the magnetic field of the two parallel wires, having a radius r, length of a single wire l, and spacing d, is given with sufficient accuracy by the formula[10]

$$L = 4l(\log_e d/r + \tfrac{1}{4}) \times 10^{-9} \text{ henries}$$

provided l is greater than $10d$ and d is greater than $10r$.

The capacitance between the wires is not of great importance in standards of low resistance, but in the case of high resistance such as used here, it becomes the predominating factor. The capacitance can be computed only when certain conditions are fulfilled which will be examined now. In general, when it is desired to compute accurately the capacitance between two conductors we must take into account their capacitances to earth or devise a means of eliminating their effects.

[10] Russel, *Alternating Currents*, Vol. 1.

Fig. 2 shows two wires in section suspended at equal distances from the earth and indicates the three capacitances which must be considered. C_{12} is the capacitance between conductors 1 and 2, and C_1 and C_2 are the earth capacitances. Grover and Curtis[1] have shown that for an important special case, the capacitance of a system such as shown in Fig. 2 is

$$C = C_{12} + C_1/2.$$

This special case requires, (1) that C_1 be equal to C_2, or that the two wires be of equal diameters and at equal distances from the earth; and (2) that V_1 be equal to $-V_2$, where V_1 and V_2 are the potentials of conductors 1 and 2, respectively. The quantity C is the capacitance in the usual sense, between the two wires and is equal to the joint capacitance of C_{12} in parallel with C_1 and C_2 in series. Orlich, who first made the analysis, gives C the name "Be-

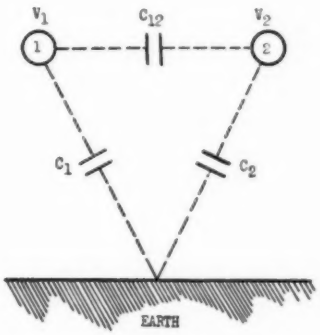

Fig. 2. A parallel wire standard in section showing the various capacitances involved.

triebskapazität" or "working capacitance." This capacitance obtains only when the condition is fulfilled that the potential of one wire is just as much above ground as the other is below, or $V_1 = -V_2$.

The working capacitance of the two parallel wires at equal distances from earth is[10]

$$C = \frac{Kl \times 10^{-6}}{3.6(\log_e (d/r) - d^2/4h^2 + d^4/32h^4 + \cdots)} \text{ microfarads}$$

where K is the dielectric constant of the medium; l the length of each wire; r the radius of the wires; d the distance between centers of wires; and h the height of wires above ground. The correction terms in d/h are usually negligible provided $h > 10\,d$.

The contribution to the effective inductance of the standard by the working capacitance C is not $-CR^2$ but $-CR^2/3$ approximately. This is occasioned by the fact that one pair of ends of the parallel wire standard are joined together, and therefore the voltage between the wires varies from zero at the closed end to the total voltage across the standard at the open end. C is the capacitance which would be measured if the two wires were discon-

nected at the far end. The rigorous expression for the impedance of a standard with one pair of ends joined is[11]

$$Z = \left(\frac{R + i\omega L}{i\omega C}\right)^{1/2} \tanh\left[i\omega C(R + i\omega L)\right]^{1/2}.$$

Since both C and L are small this may be expanded into a rapidly converging power series

$$Z = (R + i\omega L)\left[1 - (\tfrac{1}{3})i\omega C(R + i\omega L) + (2/15)i\omega C(R + i\omega L) + \cdots\right]$$

where i is the complex operator and ω is $2\pi \times$frequency. Dropping terms involving the product of C and L or their squares, this becomes

$$Z \leqq R + i\omega(L - CR^2/3).$$

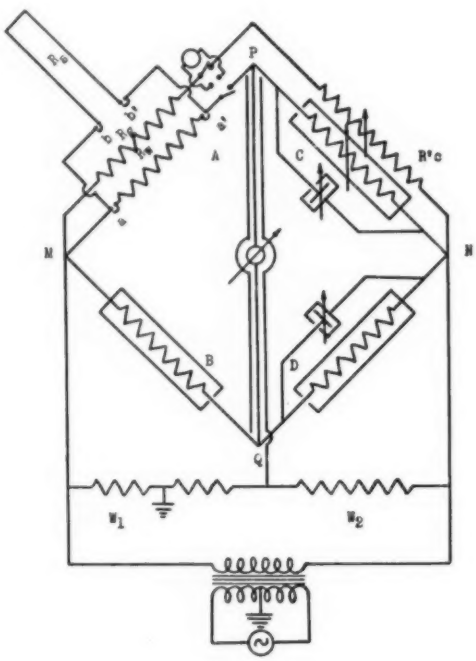

Fig. 3. The circuit for measuring the phase angle of an ideally shielded resistor.

Thus, it is seen that the effective inductance of a standard as used here is

$$L' = (L - CR^2/3)$$

where L and C are computed by use of the formulas given above.

4. Description of the Bridge Circuit

A schematic diagram of the circuit used in the measurement of the phase angle of the ten thousand ohm ideally shielded resistor is shown in Fig. 3.

[11] B. Hague, *A.C. Bridge Methods*, 2nd Edition, p. 37.

The circuit used for the units of lower resistance was essentially the same with the exception that the equal arm bridge was departed from. The basic elements of the bridge reduce to an ordinary four arm network. The other arms are added merely to maintain the shielding at the proper potentials and to furnish a convenient ground for the circuit. As previously mentioned this is a substitution method where the substitution is carried out in arm A.

Referring to Fig. 3, R_w represents the working coil of the unit whose phase angle is to be measured. R_w can be inserted into or removed from the circuit by means of the links aa' which fit into the mercury wells. The shielding resistance R_g, which completely surrounds R_w, is always in the circuit and is connected in series with a variable resistance R_c'. R_g and R_c' in series are connected directly across the source. The parallel wire standard, R_S, is so arranged that it can also be inserted in or removed from arm A by the use of links bb'. Arm B contains a fixed shielded resistor having an ohmic value of 10,000; the shield is connected to one side of the source. Arm D consists of another 10,000 ohm shielded resistor which has connected in parallel with it a variable air capacitor. Both the shield of the resistor and that for the capacitor are connected to the other side of the source. Arm C contains a variable shielded resistor of the decade type which is also shunted by a variable air capacitor with maximum capacitance of 250 mmf. This resistance box is equipped with six decades of resistance one of which permits a variation of resistance as small as 0.01 ohm, the total being 10,000 ohms.

W_1 and W_2, which are commonly known as the Wagner arm, were made up of three tube rheostats adjusted by means of a Wheatstone bridge to one-tenth the resistance of the arms B and D across which this arm is shunted. The purpose of the Wagner arm is to maintain the detector shielding at a potential equal to that of the detector lead within it and also makes possible the grounding of the bridge at the proper point. In order to make the phase relations of W_2 the same as those of arm D of the bridge it should be shunted by a capacitor. It has been found both experimentally and mathematically by W. B. Kouwenhoven and A. Banõs[12] that a small unbalance as to the phase of the shielding potentials produces a negligible effect on the main bridge, provided the insulation resistance between the shield and the lead it contains is infinite. Furthermore, even if the potential of the detector shield should differ a small amount in phase from that of the detector lead no error is introduced since arms B and D remain fixed during the substitution process as well as the Wagner arm. Thus, the omitting of a capacitor across W_2 is doubly justified.

W_1 is divided into two parts and at the junction of these the bridge is grounded. This in effect places the midpoint of the parallel wire standard, R_s, at ground potential without actually grounding the standard itself. Thus, the condition is fulfilled that one wire of the standard be just as much above ground potential as the other is below it, which permits the calculation of the capacitance of the standard. This brings about a balance in the capaci-

[12] W. B. Kouwenhoven and A. Banõs, Jr., *A High Sensitivity Power Factor Bridge*, A.I.E.E Trans. **51**, 202 (1932).

tance currents to earth just as was the case in the shielded resistor illustrated by Fig. 1B.

In order to facilitate the adjustment of the currents in the shielding coil and the working coil of the resistors, provisions were made so that a milliammeter could be inserted in series with either by the use of a simple switching arrangement. The current in R_w was adjusted by varying the voltage on the bridge and that in R_g by varying R_c'.

The alternating e.m.f. was supplied to the bridge through a two-to-one step-up transformer. The midpoint of the primary was grounded to eliminate capacitance effects from the source. Measurements were made at two frequencies, namely 500 and 60 cycles. A small aeroplane generator served as a 500 cycle source, and a regular 60 cycle alternator, driven by a direct current motor supplied from a storage battery, furnished the 60 cycle e.m.f. At 500 cycles a Baldwin telephone receiver unit of approximately 1700 ohms resistance was used as the detector. The telephone unit was completely shielded by means of a metal container which was connected to the shielding of the detector leads. The effects of earth capacitance to the observer were avoided by listening at the far end of a piece of rubber tube, the other end of which was connected to the diaphragm chamber. For the 60 cycle measurements a high resistance (850 ohms), high current sensitivity (0.25 microamperes per cm at a meter scale distance) vibration galvanometer served as a detector. This instrument was recently developed by the Leeds and Northrup Company. The balance was detected by means of a telescope placed five meters from the galvanometer.

Measurements were made on three of these ideally shielded resistors, ranging from 1000 to 10,000 ohms. Fig. 3 gives the circuit for the 10,000 ohm unit where the resistance in each arm of the main bridge is approximately 10,000 ohms. For measurements on the other two units the circuit was modified only slightly. Arms C and D were always left the same as well as W_2 of the Wagner arm. The appropriate standard of very nearly the same resistance as that of the unknown, together with the unknown, were placed in arm A so that one could be substituted for the other. The resistance in arm B was made approximately equal to that of the unknown. The resistance of W_1 was adjusted to one-tenth that of arm B. The ground was always placed at the midpoint of W_1 to bring the midpoint of the standard to ground potential.

In making the measurements the bridge arms B and D (Fig. 3) remained fixed throughout the substitution process. The capacitor in arm D was used merely as a ballast to bring the reading of that in arm C to a convenient part of the scale. The unknown and the standard were alternately inserted in arm A, and a balance was obtained each time by adjusting the resistance and capacitance of arm C only. If the resistance of the standard is adjusted closely to that of the unknown the required change in resistance of arm C during the substitution process is so small that the change in the residual effective inductance of this resistance is negligible. No particular care need be exercised in adjusting the resistance of the standard to the same value as that of the unknown when the effective inductance of the resistance of arm C is known

for every setting by a previous measurement. This phase angle can easily be taken into account in the computations as will be shown.

5. Theory of the Bridge Circuit

In the solution of the bridge equation the following notation is used: R_s is the resistance of parallel wire standard; L_s the effective inductance of parallel wire standard; R_w the resistance of working coil of unknown; L_w the effective inductance of unknown. R_σ and C_σ are the resistance and capacitance respectively, required in arm C to obtain a balance with the standard in circuit. R_ω and C_ω are the resistance and capacitance respectively, required in arm C to obtain a balance with the unknown in circuit. L_σ is the effective inductance corresponding to setting R_σ in arm C. L_ω is the effective inductance corresponding to setting R_ω in arm C; i the complex operator; $Z_a = R_w + i\omega L_w$, or $R_s + i\omega L_s$; $Z_b = R_b$;

$$Z_c = \frac{R_\omega}{1 + i\omega C_\omega R_\omega} \quad \text{or} \quad \frac{R_\sigma}{1 + i_\omega C_\sigma R_\sigma}$$

$$Z_d = \frac{R_d}{1 + i\omega C_d R_d}.$$

Now for zero current through the detector, we have

$$Z_c/Z_a = Z_d/Z_b = \text{constant} \tag{1}$$

where the subscripts refer to the various arms of the bridge of Fig. 3. Eq. (1) is equated to a constant because Z_d and Z_b remain unaltered during the measurement. Hence, we can equate the ratio of Z_c to Z_a with the standard in the circuit to the same ratio with the unknown in the circuit. Doing this we have

$$\frac{Z_c}{Z_a} = \frac{R_\sigma}{1 + i\omega C_\sigma R_\sigma} \frac{1}{R_s + i\omega L_s} = \frac{R}{1 + i\omega C_\omega R_\omega} \frac{1}{R_w + i\omega L_w}. \tag{2}$$

Solving for L_w, we obtain the formula which is used to compute the effective inductance of the unknown in terms of the known constants of the circuit,

$$L_w = R_\omega(L_s/R_\sigma + R_s C_\sigma - R_w C_\omega), \tag{3}$$

a result sensibly independent of the frequency.

In the above analysis it was tacitly assumed that the resistance in arm C has no phase angle which is not true. But, since this phase angle enters as that of the difference of two settings which are nearly equal when the resistance of the standard is adjusted closely to that of the unknown, Eq. (3) is true for this special case. If, however, the phase angle of the resistance of arm C is known, Eq. (3) can be made general by adding two correction terms. In the latter case it is not essential to adjust R_s closely equal to R_w. With the addition of the correction terms Eq. (3) becomes,

$$L_w = R_\omega[L_s/R_\sigma + (R_s C_\sigma + L_\sigma/R_\sigma) - (R_w C_\omega + L_\omega/R_\omega)] \tag{4}$$

where L_σ and L_ω must be obtained from previous measurements on the resistance in C.

6. Precautions Observed in Measurements

In the measurement of such minute quantities as are involved here, extreme care must be exercised to avoid the introduction of errors comparable in magnitude with the quantity to be measured. A small movement of any of the leads in the bridge proper is sufficient to give rise to a large error. To guard against this all leads were rigidly fastened. The effect of capacitance to the observer from the detector or the main bridge arms is sufficient to give rise to a similar error. This required careful shielding of the detector and bridge arms as well as remoteness of the observer from the detector. With proper shielding a movement of the observer merely changes the capacitances of the shields to earth and its only effect is a change in the load on the source. When the telephone detector already described was used listening was done at the end of a five foot rubber tube. The 60 cycle detector was at a distance of more than five meters from the observer and balance was detected by the use of a telescope.

The Wagner arm, W_1 and W_2, may be another troublesome cause of error if improperly placed. During the course of the development of this method, the Wagner arm and source were connected to the points P and Q and the detector to points M and N instead of as shown in Fig. 3. Hence, the Wagner arm, instead of being across the fixed arms B and D, was across two arms, one of which is varied in the substitution process. When C is changed, the Wagner arm remaining fixed, it is evident that the potential of the detector lead is shifted with respect to the potential of its shield. Also, a few ohms change in C will shift the point on the bridge which is at ground potential. These two disturbances were responsible for inconsistent results which at first were found difficult to account for. Therefore, it may be said that the bridge will operate satisfactorily only when the Wagner arm is in the position indicated in Fig. 3.

The success of this method depends on the use of a relatively high voltage as a source. A high voltage was especially necessary at 60 cycles in order to obtain the required sensitivity. The limiting factor in raising the voltage was the current carrying capacity of the parallel wire standard. The voltage could not be carried above 300 volts without obtaining annoying fluctuations due to heating in the standard.

Check on accuracy

In order to check the overall accuracy of the set-up two parallel wire standards of the same resistance but with different spacings were constructed. The spacing between wires of one of these was 1 cm and that for the other was 20 cm. This may be said to represent two extremes of spacing. The effective inductance of an arbitrarily chosen shielded resistor of considerably higher phase angle than may be expected of the ideally shielded resistor, was measured first by using one of these two standards and then the other. The resistor was of the type illustrated in Fig. 1B and possessed an effective inductance of approximately -0.9 mh for a 10,000 ohm unit. The circuit of Fig. 3 was adapted to this resistor by replacing R_w with it and omitting R_g

and R_c'. The shield was connected to the ground point of the Wagner arm which fixes the potential of the shield and makes it equal to that of the midpoint of the resistance within it. In this preliminary test the effective inductance as obtained from the two sets of data differed by less than ten percent, or a time constant of less than 10^{-8} seconds. This may be looked upon as a good agreement, considering the severity of the test and the smallness of the time constant (9×10^{-8} sec.). A large portion of the discrepancy in the results obtained with the two standards was probably due to errors involved in the measurements of the physical dimensions of the standards.

For the purpose of gaining a more definite idea as to the magnitude of such errors, liberal uncertainities were assumed in the measurement of dimensions of the standard. Two complete computations of the effective inductance were carried through with such values as would give the extreme difference in the final result. For the one centimeter spacing the discrepancy between the two extremes was found to be about four percent of the total effective inductance of the standard. In a similar computation for the 20 cm spacing it was found to be only one percent. The difference in the two cases is mainly due to the accuracy with which the spacing can be measured. It is reasonable to assume that a 20 cm spacing can be measured with greater relative accuracy than a 1 cm spacing. These computations, therefore, indicate the importance of measuring the physical dimensions of the standards accurately and especially the spacing between wires.

7. Measuring Procedure

Since the ideally shielded resistors were constructed so that the resistance of the shielding coil is equal to that of the working coil, a minimum of effective inductance may be expected when the currents through the two coils are equal. Actually, this is not quite the case because of end-effects, and the always existing self-inductance and self-capacitance. In order to gain some definite information as to the nature of the variation of the effective inductance of the working coil with variation of the current through the shielding coil, a series of measurements was made in which the current through the shielding coil was changed from zero to approximately twice the fixed current through the working coil. The current through the working coil is determined by the maximum permissible voltage on the bridge commensurate with heating. The current through the shielding coil was adjusted to any desired value by varying the resistance R_c' which possessed a range of from 1 to 100,000 ohms.

It might be mentioned here that the resistance of the milliammeter used was of the order of several hundred ohms, and thus small compared to the resistance of the bridge arms with which it was connected in series to measure the current. This method of measuring the current was accurate enough for the purpose in hand.

Again referring to Fig. 3, with R_w in circuit and the standard disconnected, the current through R_w was brought up to a fixed value by increasing the voltage on the bridge. Then the current through R_g is adjusted to the desired

value by varying R_c'. This being done, the milliammeter is taken out of the circuit, and a balance is then obtained by use of the resistance and capacitance in arm C. It may be found necessary to adjust the capacitor in arm D to bring the balance point of the capacitor in arm C to a convenient part of the scale. Once the latter adjustment is made arms B and D are left untouched. This balance results in a resistance reading R_ω and a capacitance reading C_ω in arm C according to the notation used. Now by the use of links aa' and bb', R_w is taken out of the circuit and the standard is inserted. The circuit is again balanced using arm C only, giving a resistance reading R_σ and a capacitance reading C_σ. Knowing the resistance of the coil under test and that of the standard we now have enough data to compute the effective inductance by use of formula (3).

The resistors were tested at two frequencies, 60 and 500 cycles per second. At a frequency of 500 cycles per second measurements were made for a series of values of current through the shielding coil, on all three of the units. A number of measurements were made on the 10,000 ohm unit and also the 5000 ohm unit at 60 cycles. Since the measurements at 60 cycles on the 5000 ohm unit were obtained with difficulty due to low sensitivity, no attempt was made to obtain 60 cycle measurements on the 1000 ohm unit.

8. Results for Ideally Shielded Resistors

The data obtained on the three units are listed in the tables below. Standards with 20 cm spacing were used. The first column of the tables is headed I_w, the current through the working coil, and the second is headed by I_g, the current through the shielding coil. The other columns are headed by symbols whose meaning has already been explained.

The last column of the above three tables gives the effective inductance as observed for various currents through the shielding coil. These values are listed to the nearest hundredth millihenry, since computation to a greater degree of accuracy is not justified in measurements on resistances of the order of magnitude dealt with here. The individual figures set down in the table

Table I. *10,000 ohm unit.*

I_w m.a.	I_g m.a.	R_ω ohms	C_ω mmf	R_σ ohms	C_σ mmf	L_w mh
			500 cycle measurements			
10.6	0	9930	77.9	9982	68.7	−1.44
10.6	2.65	9930	80.2	9982	74.4	−1.10
10.6	5.30	9930	74.8	9982	73.4	−0.67
10.6	7.95	9930	68.8	9982	70.4	−0.37
10.6	10.60	9930	69.2	9982	74.1	−0.04
10.6	13.25	9931	57.0	9983	65.8	+0.34
10.6	15.90	9931	52.7	9983	64.1	+0.60
10.6	18.55	9931	44.2	9983	60.8	+1.01
			60 cycle measurements			
10.6	7.95	9929	63.2	9982	63.8	−0.47
10.6	10.60	9929	56.4	9982	61.0	−0.08
10.6	13.25	9929	48.8	9983	58.7	+0.45

TABLE II. *5000 ohm unit.*

I_w m.a.	I_g m.a.	R_ω ohms	C_ω mmf	R_σ ohms	C_σ mmf	L_w mh
			500 cycle measurements			
12.0	0.0	9934	80.4	9970	76.8	−0.25
12.0	3.0	9934	84.3	9970	81.2	−0.22
12.0	6.0	9934	81.5	9970	80.2	−0.13
12.0	9.0	9933	79.1	9970	79.3	−0.06
12.0	12.0	9935	70.0	9973	71.4	0.00
12.0	15.0	9936	65.3	9973	68.0	+0.06
12.0	18.0	9936	66.0	9973	70.3	+0.14
12.0	20.0	9933	69.3	9970	75.2	+0.22
			60 cycle measurements			
12.0	12.0	9932	60.5	9964	61.3	−0.04
12.0	15.0	9933	57.9	9964	59.7	+0.01

TABLE III. *1000 ohm unit, 500 cycle measurements.*

I_w m.a.	I_g m.a.	R_ω ohms	C_ω mmf	R_σ ohms	C_σ mmf	L_w mh
12.0	0.0	9981	64.5	9997	61.9	−0.01
12.0	3.0	9981	64.5	9997	62.5	−0.01
12.0	6.0	9981	62.5	9997	61.0	0.00
12.0	9.0	9981	63.3	9997	62.1	0.00
12.0	12.0	9981	61.5	9997	60.4	0.00
12.0	15.0	9981	60.9	9997	59.7	0.00
12.0	18.0	9981	63.3	9997	62.9	+0.01
12.0	20.0	9981	63.0	9997	62.3	+0.01

represent the average of from five to ten separate measurements. The resistance balance changed only slightly, because of heating in the standard, during a series of measurements. The individual capacitance balances, however, were subject to some variations. In the case of the 10,000 ohm unit the average deviation from the mean at 500 cycles for ten capacitance readings was approximately one percent. At 60 cycles, however, the average deviation from the mean for the same number of readings was seven percent. For the other two units this variation was still quite small at 500 cycles, not exceeding two percent; but at 60 cycles it mounted to about 10 percent for the 5000 ohm unit. No 60 cycle measurements were attempted on the 1000 ohm unit, for the limit of sensitivity of the detector was approached in the measurements on the 5000 ohm unit. Since the 60 cycle measurements agreed closely with the 500 cycle measurements for the two higher resistance units, it is reasonable to assume that the same would have been true for the 1000 ohm unit. The sensitivity at 500 cycles was sufficient to measure time constants of the order of 10^{-8} seconds to a fair degree of accuracy, even for the 1000 ohm unit where the results were consistent to within two percent.

The curves of Fig. 4 illustrate the nature of the variation of the effective inductance with the variation of the current I_g, through the shielding coil, for the three units. It is seen to be linear with I_g as may be expected, and changes from negative to positive as I_g is increased from zero. The slope of

the curves have been found to be directly proportional to the product of the distributed capacitance between the two coils and the resistance. Silsbee[8] found a similar result for resistors of the type illustrated by Fig. 1B. The point on each of the curves of Fig. 4 where the two currents are equal are marked by leaders. This point is the most important, even though the phase angle is not quite zero, because it represents the conditions under which the resistor is used in practice.

The change of sign of the effective inductance is due to the reversal of the direction of capacitance currents between the two coils. When the current in the shielding coil is less than that in the working coil, the potential of any point on the shielding coil is lower than that of a corresponding point on the

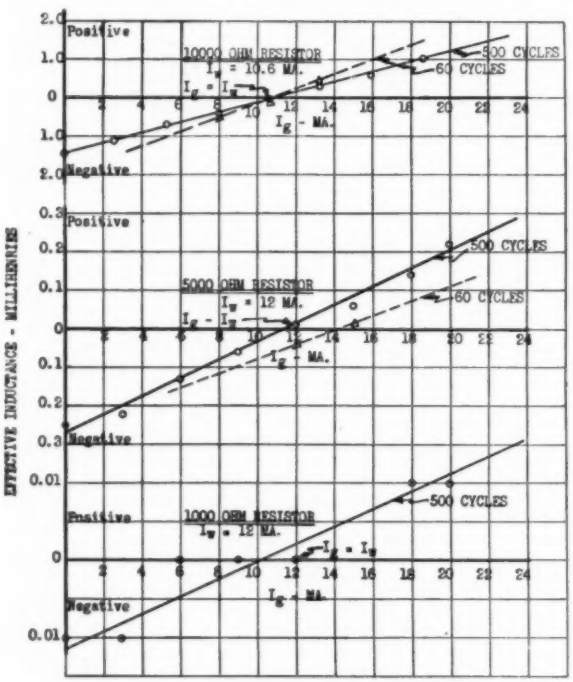

Fig. 4. Curves showing the variation of effective inductance with the variation of the current through the shielding coil for the three ideally shielded resistors.

working coil. Therefore, the capacitance current passes from the working coil to the shielding coil. Now, when I_g is greater than I_w, the potential of any point on R_g is higher than that of a corresponding point on R_w, and thus the capacitance current passes from R_g to R_w. This reversal of capacitance currents corresponds to a phase change of 180° and hence accounts for the change of sign of the effective inductance.

In Fig. 4 it will be noted that the effective inductance at the point $I_g = I_w$ becomes increasingly more positive as the resistance of the unit decreases. It is still slightly negative for the 10,000 ohm unit but becomes decidedly positive for the 1000 ohm unit. It will be further noted that the agreement

between the results at the two frequencies, though close in all cases, becomes less close as the resistance of the unit decreases. This is explained by the fact that in the lower resistance units the effect of self-inductance becomes appreciable compared to the capacitance effects. In the 10,000 unit the self-inductance is extremely small compared to the capacitance and therefore the curves at the two frequencies almost coincide.

Since the values of the phase angle with equal currents through the two coils are the ones in which we are most interested, they are set down in Table IV as computed for a frequency of 60 cycles. The agreement between the results at the two frequencies was close enough to justify taking the simple average of the two sets of data where measurements were made at two frequencies.

TABLE IV.

Resistor	L_w	Phase angle $=\theta$	Tan $\theta=\theta$
10,000 ohm	−0.06 mh	−0.47 sec.	−0.0000022 rad.
5000 ohm	−0.02 mh	−0.31 sec.	−0.0000015 rad.
1000 ohm	+0.005 mh	+0.19 sec.	+0.0000019 rad.

Referring to Table III it is seen that the effective inductance for equal currents in the two coils of 1000 ohm unit is set down as zero. This simply means that the value is less than 0.005 mh, since computations were made to the nearest 0.01 mh. Although the error in measurement was probably only a fraction of 0.01 mh, computation to a higher degree of accuracy was not necessary in this work. The purpose of the measurements on these shielded resistors was to show that the phase angle is less than 10^{-5} radians, or, that the time constant is less than 10^{-7} seconds. 0.01 mh, even for the 1000 ohm unit, which is the worst case, corresponds to a time constant of 10^{-8} seconds, which is negligible for all but the most precise measurements. By drawing an average straight line for the points obtained for the 1000 ohm unit, Fig. 4 indicates that the effective inductance is decidedly positive and less than +0.005 mh for the point $I_g = I_w$. Thus, the value +0.005 mh set down in Table IV for the 1000 ohm resistor is probably larger than the actual value. This corresponds to a time constant of 5×10^{-9} seconds.

9. EXTENSION OF THE RANGE FOR THIS METHOD

In the preceding pages it has been shown quite conclusively that the circuit gives consistent results for resistances ranging from 1000 ohms to 10,000 ohms and can be used to measure time constants as small as 10^{-8} seconds with a fair degree of accuracy. The type of shielded resistances upon which these measurements were made may be said to possess the lowest phase angle of any shielded resistor found in practice and thus the most difficult to measure. Even more satisfactory results may be expected in measurements on other types of shielded resistors. By obvious and very simple modifications the circuit may be adapted to either of the other two types of shielded resistors illustrated in Fig. 1.

The upper limit of this circuit is not 10,000 ohms but has been used by the writer for resistances up to 50,000 ohms. Since parallel wire standards having a resistance of more than 10,000 ohms become quite long, measurements were carried out on the higher resistances in a slightly different manner, in which a number of 10,000 ohm shielded resistors were necessary. The effective inductances of several 10,000 ohm resistors are measured separately using the 10,000 ohm standard. Once the effective inductance is known the appropriate number of 10,000 ohm resistors can be connected in series and the combination used as a secondary standard replacing the primary parallel wire standard.

Fig. 5 gives the connections for measurements on a 20,000 ohm shielded resistor of the type illustrated in Fig. 1B. Arms C, D, and W_2 are always left

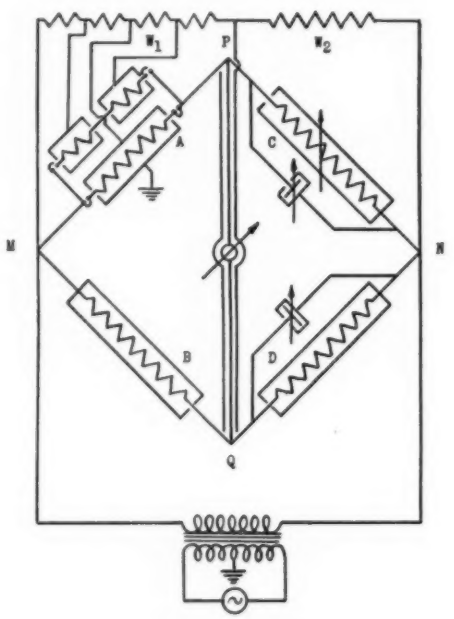

Fig. 5. Circuit for comparing the phase angles of resistors.

the same as in Fig. 3. The resistance of arm B is made approximately equal to that of the unknown in arm A. W_1 is made one-tenth that of arm A. The two resistances in the upper part of arm A are previously measured with the 10,000 ohm standard. The two are connected in series and the resultant effective inductance of the series connection is the sum of those for the individual units. With the series connection of units as a secondary standard, the effective inductance of the 20,000 ohm unit is measured in exactly the same manner as that for a 10,000 ohm unit. The shields of the various units in arm A are maintained at the proper potential by connecting them to W_1 as indicated in Fig. 5. It has been found that with this circuit it is immaterial where the ground is placed, but to be consistent it was always connected to the midpoint of W_1.

By the use of a series connection of units the circuit has been used with good sensitivity both at 500 and 60 cycles for resistances as high as 50,000 ohms. As the magnitude of the resistance increases, however, the voltage must be raised to get the required sensitivity. For 50,000 ohm resistors about 500 volts had to be used in order to get good results at 60 cycles.

The circuit can also be used to measure the phase angle of ordinary shielded resistance boxes. For precise measurements such as the measurement of power factor of dielectrics, the phase angle of the average resistance box is not always negligible. The effective inductance of a 10,000 ohm box made by a well-known manufacturer has been found to be -2.54 millihenries. This corresponds to a phase angle of -0.33 min. at 60 cycles. Before making the measurement the box was shielded in a manner illustrated in Fig. 1A.

10. Summary

The small, but not always negligible phase angles of "non-inductive" shielded resistors are often ignored because of the supposed extreme difficulty of their measurement. The substitution method described in detail can be carried out without the use of any very special apparatus with the exception that it must be possible to vary the resistance of the box in arm *C* of Fig. 3 by as little as 0.01 in 10,000 ohms. The use of only one arm of the bridge network in balancing, and the use of an air capacitor to balance for phase, makes it a simple matter to eliminate the effect of parasitic influences. The air capacitor as used here is subject to no parasitic effects. The measurements on the ideally shielded resistors prove conclusively that consistent results can be obtained with an accuracy sufficient for the most precise measurements in which such resistors may be used. Time constants as low as 10^{-8} seconds were measured with a fair degree of accuracy.

The circuit is easily adaptable to all types of resistors. By the use of several resistors as secondary standards the range of the circuit can be extended to 50,000 ohms. The circuit can also be used to measure the phase angles of resistance boxes. The average resistance box has an inherent phase angle of sufficient magnitude to be of importance in many precise measurements.

It may be said, therefore, that the circuit described herein affords a comparatively simple means of measuring the phase angles of resistances ranging from 1000 ohms to 50,000 ohms. For frequencies as low as 60 cycles this range is narrowed slightly; it being from 5000 to 50,000 ohms.

11. Acknowledgment

The writer wishes to take this opportunity to express his appreciation to Dr. W. B. Kouwenhoven of The Johns Hopkins University for his interest in this work, to Dr. F. B. Silsbee, of the Bureau of Standards, for his many suggestions, and to Dr. F. K. Harris, also of the Bureau, for his helpful advice and active assistance in the work.

Dielectric Constant and Particle Size

By J. W. Williams and J. L. Oncley
University of Wisconsin

(Received September 22, 1932)

ONE OF the achievements of modern physical science is the success with which the structure of atoms and molecules has been elucidated. It has been possible to assign definite structures to a number of the simpler molecules and to determine the molecular weights of an enormous number of more complicated ones. However, serious difficulties arise when it becomes necessary to associate a definite weight with the complex molecules or other structural units which form such important substances as rubber, cellulose, body tissue, protoplasm, gelatin, glue, haemoglobin, egg albumin, synthetic resins, wool, silk, and the cellulose esters. The scientist and technician must now use these materials without having much information about their structures.

In spite of these difficulties modern physical studies are revealing the size and weight of the more elementary units of the structures, and the manner in which they are arranged to form the massive substance. It is with the first of these problems that we are interested. A successful method to determine the micellar or particle weight of such substances consisting of spherical molecules or particles has been developed by Svedberg and his associates. It consists of a study of the velocity with which a particle whose weight or size is to be determined sediments in a centrifugal field of known force. The tendency of the particle to settle out in such a field is opposed by the linear frictional resistance offered to its movement in a viscous medium in which it is suspended. Well-known laws enable us to calculate the size of a sedimenting particle since the force of the centrifuge just overcomes the force of friction when the particle falls with a constant and measurable velocity.

Another method by which the size and therefore the weight of a spherical particle can be determined requires experimental data of quite another type but at the same time embodies certain similar principles. It has recently been described by Marinesco,[1] and independently but somewhat later by Williams and Oncley.[2] It is an application of the dipole theory of Debye and depends upon the fact that because of the frictional resistance of the medium to the rotation of a suspended particle a finite time is required for its orientation in an alternating electrical field. According to this theory it follows that if the frequency dependence of the dielectric constant is determined for a system composed of electrically dissymmetrical particles suspended in a liquid me-

[1] (a) Marinesco, Comptes Rendus **189**, 1274 (1929); see also Conference-communication faite a la Soc. de Chimie-physique de France. Seance du 26 juin 1929; (b) J. chim. Phys. **28**, 51 (1931); (c) Kolloid Zeits. **58**, 285 (1932).

[2] (a) Williams, J. Frank. Inst. **211**, 581 (1931); (b) Williams and Oncley, J. Rheology **3**, 271 (1931).

dium there will be found to be a region in which the dielectric constant decreases as the frequency is increased. The size and therefore the weight of the suspended particle is expressed in terms of the dielectric constants for zero and for infinite frequencies, and either the time of relaxation or the true inner frictional coefficient of the liquid.

The *qualitative* argument may be briefly stated by saying that at sufficiently high frequencies the dielectric constant will fall off, because the inner friction constant of the medium prevents the orientation of the dipole particles which contribute to the dielectric constant. The polarization consists of two parts, a polarization due to deformation of the particle by an adjustment of the atoms and electrons, and a polarization due to the orientation of the particle itself. The transition from both distortion and orientation effects to the distortion effect alone will occur in a frequency region defined *approximately* by the equation

$$\nu_c \tau = 1 \tag{1}$$

where τ, called the time of relaxation of the molecules, is the time required for $1/e$ of the particles to assume a random distribution after the applied field has been removed, and ν_c is the frequency of the alternating field. It should be emphasized that this equation serves only to indicate the region in which anomalous dispersion occurs, and means simply that ν_c and $1/\tau$ must be of the same order of magnitude.

In order to have the situation clearly before us it seems worth while to give an abbreviated outline of the *exact* dispersion theory as it has been given by Debye, and then to extend the theory so that it may be applied to solutions or suspensions of polar particles in dilute solution in a nonpolar solvent. It will be seen that as a result of these calculations the transition between the high and low values of the dielectric constant will take place in the frequency region defined by the expression,

$$0.1 \leqq x \leqq 10.$$

In this equation

$$x = \frac{\epsilon_0 + 2}{\epsilon_\infty + 2} \cdot \frac{\pi \zeta \nu}{kT},$$

where ϵ_0 is the dielectric constant at zero frequency, ϵ_∞ is the dielectric constant at infinite frequency, k is the Boltzmann constant, T is the absolute temperature, ν is the electrical frequency in cycles per second, ζ is the "inner-frictional constant" which, when and if Stokes' law can be applied is equal to $8\pi r^2 \eta$, η is the ordinary coefficient of viscosity of the solution and r is the radius of the particle.

If the system is a polydisperse one the curves obtained when either of the dielectric constants (real or imaginary) or the power factor are plotted against the frequency will be flattened out. They may be regarded as the result obtained when the simple curves for the several particle sizes are added together.

The treatment of Debye[3] resolves itself into a consideration of the generalized distribution of the dipole moments of the polar molecules if affected by an alternating electrical field. Saturation effects do not enter in because the field strengths used in the ordinary experiments are small. The case of a field of force in one direction only in which the field is variable with time but constant in direction is considered sufficient for the dispersion problem. If we now suppose a spherical surface drawn in the liquid and take the center of this sphere as the pole of our polar coordinate system, then obviously the distribution function for the dipole moments must depend upon the polar angle θ and upon the time t. Thus the number of molecules whose moments point in the direction of a solid angle $d\Omega$ at a given time can be denoted by $fd\Omega$ where f is $f(\theta, t)$.

Let us consider the events taking place during an interval of time δt. If $t=0$ at the beginning of this interval at the end of it we will have $t=\delta t$. Let us further assume that δt is sufficiently large for all molecules whose moments were in $d\Omega$ at $t=0$ to have shifted outside this angle when $t=\delta t$, and yet small enough so that during the time δt the moments will shift not more than a few degrees. Then the number of molecules whose moments enter $d\Omega$ in the time δt will be

$$\delta t(\partial f/\partial t)d\Omega = \Delta_1 + \Delta_2 \tag{2}$$

where Δ_1 is the contribution due to rotations produced by the impressed field, and Δ_2 is the contribution due to rotations caused by the Brownian movement.

The result of the calculations for Δ_1 and Δ_2 will be given at once:

$$\Delta_1 = -\frac{1}{\sin\theta}\frac{\partial}{\partial\theta}\left(f\cdot\frac{M}{\zeta}\cdot\delta t\sin\theta\right)d\Omega \tag{3}$$

$$\Delta_2 = d\Omega\frac{\overline{\Theta}^2}{4}\left(\frac{\cos\theta}{\sin\theta}\frac{\partial f}{\partial\theta}+\frac{\partial^2 f}{\partial\theta^2}\right). \tag{4}$$

The negative sign in the expression for Δ_1 takes account of the fact that the torque acts opposite to the direction of increasing angle θ.

In these equations the torque on a molecule is $M=-\mu F\sin\theta$, where μ is the electric moment and F is the electrical intensity acting upon one molecule or particle. The significance of Θ will be understood from the fact that the constant $\overline{\Theta}^2/\delta t$ is closely related to the well-known constant $\bar{x}^2/\delta t$ in the ordinary expression for the Brownian movement. It is the mean angular rotation squared per unit interval of time.

Substituting Eqs. (3) and (4) in (2) there results the expression

$$\frac{\partial f}{\partial t}=\frac{1}{\sin\theta}\frac{\partial}{\partial\theta}\left[\sin\theta\left(\frac{\overline{\Theta}^2}{4\partial t}\cdot\frac{\partial f}{\partial\theta}-\frac{M}{\zeta}\cdot f\right)\right]. \tag{5}$$

The constant $\overline{\Theta}^2/4\delta t$ evaluates to kT/ζ, thus,

[3] Debye, *Polar Molecules*, Chemical Catalog Co., New York, 1929. German Edition, Hirzel, Leipzig, 1929.

$$\zeta \frac{\partial f}{\partial t} = \frac{1}{\sin\theta} \frac{\partial}{\partial \theta}\left[\sin\theta\left(kT\frac{\partial f}{\partial \theta} - M \cdot f\right)\right] \tag{6}$$

which is the differential equation expressing f as a function of θ and t.

The intensity of an electrical field which is alternating periodically is given by the formula $F = F_0 \cos \omega t$ where ω is the number of vibrations in 2π seconds (vibrations in one second). For mathematical simplicity this is expressed as the real part of $F = F_0 e^{i\omega t}$. Therefore, $M = -\mu F_0 e^{i\omega t} \sin\theta$. Making the further substitution $\tau = \zeta/2kT$ Eq. (6) becomes

$$2\tau \frac{\partial f}{\partial t} = \frac{1}{\sin\theta} \cdot \frac{\partial}{\partial \theta}\left[\sin\theta\left(\frac{\partial f}{\partial \theta} + \frac{f\mu F_0 e^{i\omega t}}{kT}\sin\theta\right)\right]. \tag{6a}$$

The solution of this equation is

$$f = A\left[1 + \frac{1}{1 + i\omega\tau} \cdot \frac{\mu F_0 e^{i\omega t}}{kT}\cos\theta\right]. \tag{7}$$

The mean moment of a particle or molecule is

$$\bar{m} = \left(\alpha_0 + \frac{\mu^2}{3kT} \cdot \frac{1}{1 + i\omega\tau}\right)F. \tag{8}$$

The meaning of the complex moment is that there is a difference in phase between the dipole moment and the internal force.

Also, since $\bar{m} = \alpha F$ and $(\epsilon - 1)/(\epsilon + 2) = (4\pi/3)n\alpha$ where α is the polarizability and n is the number of polar particles per cubic centimeter, we may write

$$\frac{\epsilon - 1}{\epsilon + 2} = \frac{4\pi}{3} n\left[\alpha_0 + \frac{\mu^2}{3kT} \cdot \frac{1}{1 + i\omega\tau}\right] = P(\omega)\frac{d}{G}. \tag{9}$$

Thus, the molar polarization $P(\omega)$ and dielectric constant ϵ for a polar substance of deformation polarizability α_0, electric moment μ, density d, and molecular or particle weight G has been calculated assuming that the Clausius-Mosotti hypothesis is valid for the pure substance. However, this is known to be the case only when such polar molecules are dissolved or otherwise suspended in a nonpolar solvent medium. Accordingly it is necessary to give consideration to the adaption of these equations to such a system. The following is such a treatment for a solution in which n_2 polar molecules per cubic centimeter whose deformation polarization is $\alpha_2^{(0)}$ and whose dipole moment is μ_2 are dissolved in n_1 molecules per cubic centimeter whose deformation polarization is $\alpha_1^{(0)}$, and whose dipole moment is zero.

Thus, Eq. (9) above becomes

$$\begin{aligned}\frac{\epsilon_{12} - 1}{\epsilon_{12} + 2} &= \frac{4\pi}{3}\left[n_1\alpha_{1(0)} + n_2\alpha_{2(0)} + \frac{n_2\mu_2^2}{3kT} \cdot \frac{1}{1 + i\omega\tau_2}\right] \\ &= P_{12}(\omega)\frac{d}{f_1G_1 + f_2G_2} \\ &= \frac{\epsilon_{12}(\infty) - 1}{\epsilon_{12}(\infty) + 2} + \frac{1}{1 + i\omega\tau}\left(\frac{\epsilon_{12}(0) - 1}{\epsilon_{12}(0) + 2} - \frac{\epsilon_{12}(\infty) - 1}{\epsilon_{12}(\infty) + 2}\right).\end{aligned} \tag{9a}$$

Therefore

$$\epsilon_{12} = \epsilon_{12}' - i\epsilon_{12}'' = \frac{1 + 2P_{12}(\omega)d/(f_1G_1 + f_2G_2)}{1 - P_{12}(\omega)d/(f_1G_1 + f_2G_2)}$$

$$= \frac{1 + 2\left[\frac{\epsilon_{12}(\infty) - 1}{\epsilon_{12}(\infty) + 2} + \frac{1}{1 + i\omega\tau_2}\left(\frac{\epsilon_{12}(0) - 1}{\epsilon_{12}(0) + 2} - \frac{\epsilon_{12}(\infty) - 1}{\epsilon_{12}(\infty) + 2}\right)\right]}{1 - \left[\frac{\epsilon_{12}(\infty) - 1}{\epsilon_{12}(\infty) + 2} + \frac{1}{1 + i\omega\tau_2}\left(\frac{\epsilon_{12}(0) - 1}{\epsilon_{12}(0) + 2} - \frac{\epsilon_{12}(\infty) - 1}{\epsilon_{12}(\infty) + 2}\right)\right]} \tag{10}$$

$$= \frac{\epsilon_{12}(0) + x^2\epsilon_{12}(\infty)}{1 + x^2} - i\frac{\epsilon_{12}(0) - \epsilon_{12}(\infty)}{1 + x^2} \cdot x \tag{10}$$

where

$$x = \frac{\epsilon_{12}(0) + 2}{\epsilon_{12}(\infty) + 2} \cdot \omega\tau.$$

Thus,

$$\epsilon_{12}' = \epsilon_{12}(\infty) + \frac{\epsilon_{12}(0) - \epsilon_{12}(\infty)}{1 + x^2} \tag{11}$$

and

$$\epsilon_{12}'' = \frac{\epsilon_{12}(0) - \epsilon_{12}(\infty)}{1 + x^2} \cdot x. \tag{12}$$

In these equations the dielectric constant for the very low frequencies is designated as ϵ_0 for the pure substance and as $\epsilon_{12}(0)$ for the binary mixture. The quantities ϵ_∞ and $\epsilon_{12}(\infty)$ represent the corresponding dielectric constants for very high frequencies. The molar polarization is designated as $P(\omega)$ in order to distinguish it from that of the static case. The quantities f_1 and f_2 are the mol fractions of the two components of the system.

With these equations there may be calculated the expected behavior of any binary system in which the assumptions underlying both the law of Stokes and the Clausius-Mosotti hypothesis are fulfilled. It is necessary to obtain dielectric constant and density data for dilute solutions of the polar molecule or particle in a nonpolar solvent, and then extrapolate the results to zero concentration in order to find the behavior of the solute molecule under the assumed conditions. In making this extrapolation it is difficult to say just which value for the coefficient of viscosity η should be used. This extrapolation leads to additional difficulties if the law of Stokes cannot be applied. A detailed description of these difficulties involved in the use of the ordinary coefficient of viscosity and Stokes' law for calculating molecular sizes from dispersion data has already been given by us[2b] so it is not necessary to discuss them at this point.

The first application of the dipole theory to the study of colloidal chemistry was probably made by Errera.[4a] In 1928 Wo. Ostwald[4b] began the investigation of the relationship of dielectric constant, polarization and electric

[4a] Errera, Kolloid Zeits. **32,** 157, 240, 273 (1923).

[4b] Wo. Ostwald, Kolloid Zeits. **45,** 56 (1928), and a number of later interesting articles.

moment to the stability of a large number of dispersed systems. Shortly afterward Marinesco[1a] recognized that the dipole theory could be used to determine micellar size, (grandeur), and to explain a number of peculiarities observed by him during the course of his previous studies of the dielectric constant of various gelatin solutions. In the short note published in Comptes Rendus he states that "the anomalous dispersion of the dielectric constant of a colloidal solution whose micells have permanent moments permits the determination of the molecular volume, inasmuch as the time of relaxation of a micell is given by

$$\tau = 4\pi\eta_0 r^3/kT = \lambda_0/\bar{c}$$

where η_0 is the coefficient of viscosity, $\bar{c}$ is the velocity of light and λ_0 is the wave-length corresponding to the *beginning of the fall of the dielectric constant of the solution* toward the region of the anomalous dispersion, and is determined by the measuring circuit. The molecular volume in solution is

$$V = Mv = \frac{4}{3}\pi r^3 \cdot N = \frac{1}{3}\,\frac{\lambda_0}{\bar{c}}\,\frac{RT}{\eta_0}$$

where R is the gas constant and M is the molecular weight." By defining λ_0 as the wave-length corresponding to the beginning of the fall of the dielectric constant of the solution Marinesco has clearly recognized the fact that a quantitative result cannot be obtained using the expression $\nu_c\tau = 1$ or any equation equivalent to it. The point at which the dielectric constant begins to fall will certainly be difficult to locate with any degree of exactness. It may best be done by the use of the formula for the dielectric constant which marks the beginning of dispersion,

$$\epsilon = \frac{\epsilon_0 + 4\pi^2\epsilon_\infty[(\epsilon_0 + 2)/(\epsilon_\infty + 2)]^2}{1 + 4\pi^2[(\epsilon_0 + 2)/(\epsilon_\infty + 2)]^2}.$$

In his more recent publications[1b,1c] Marinesco has apparently considered it unnecessary to apply the exact relationships. Thus in the first of these articles[1b] the expression for the molecular weight of a colloid is given as,

$$M = \frac{1}{3}\,\frac{\lambda_A}{\bar{c}}\,\frac{RT}{v\eta_0}$$

and λ_A is clearly indicated in an accompanying figure to be the wave-length at which

$$\epsilon = (\epsilon_\infty + \epsilon_0)/2.$$

This is equivalent to the assumption that $\nu_c\tau = 1$, discussed above. In the determination of the molecular weight of gelatin Marinesco has worked with a 0.1 percent solution at $p_H = 3.5$. At $\lambda = 6.5$m, the dielectric constant was found to be 86.0, while at $\lambda = 1.9$m the value was less than that of pure water. Experiments at $\lambda = 6.2$m showed that the dielectric constant value had decreased to 82.5. Assuming with him that the "region of anomalous dispersion

is consequently 'very nearly' the wave-length $\lambda = 6\text{m}$" the molecular weight is found to be 11,300. A previous determination of v, a quantity necessary for the calculation, had given 1.294 cm³. This result is compared with one reported by Cohn,[5] $M = 10{,}300$, which had been obtained in solutions of like concentration, but using other methods.

The second of these articles, whose purpose is to review previous work, contains equally definite statements with respect to which objections may be raised. Thus it is stated that the dielectric constant curve passes through a point of inflection (Wendepunkt) for a wave-length λ_0' corresponding to the time of relaxation τ_1, of the dissolved molecule, and that in this instant the period of the applied field is equal to τ_1; thus

$$\lambda_0'/\bar{c} = 4\pi r^3\eta_0/kT$$

and

$$M = \frac{1}{3}\,\frac{\lambda_0'}{\bar{c}}\,\frac{RT}{v\eta_0}.$$

In spite of the fact Marinesco did not trace the exact course of the dispersion of the dielectric constant, λ_0' is now assigned the value 6m, and the gelatine is again found to have the molecular weight 11,300.

But it can be seen from Eqs. (11) and (12) that the real dielectric constant ϵ' will take on a mean value and the imaginary dielectric constant ϵ'' will pass through a maximum at the point where $x = 1$. Under these conditions

$$\frac{\epsilon_0 + 2}{\epsilon_\infty + 2}\cdot\frac{\pi\zeta\nu_c}{kT} = 1. \tag{13}$$

In other words the critical frequency ν_c is given by the relation

$$\nu_c = \frac{\epsilon_\infty + 2}{\epsilon_0 + 2}\cdot\frac{kT}{\pi\zeta} = \frac{\epsilon_\infty + 2}{\epsilon_0 + 2}\cdot\frac{1}{2\pi\tau} \tag{13a}$$

or

$$\nu_c\tau = \frac{\epsilon_\infty + 2}{\epsilon_0 + 2}\cdot\frac{1}{2\pi}. \tag{13b}$$

Eq. (13) is the exact equation which should always be used in work of this sort. The equation for the molecular or particle weight should therefore be written in the form

$$M = \frac{1}{3}\,\frac{\epsilon_\infty + 2}{\epsilon_0 + 2}\cdot\frac{\lambda_c}{2\pi\bar{c}}\cdot\frac{RT}{\eta v}. \tag{14}$$

If one recalculates the result of Marinesco for the particle weight of gelatin (dielectric constant data from dilute solution at $p_H = 3.5$) using our formula (14) it is found that the value may be of the order of magnitude 1/10 of that previously reported.[1] Thus the excellent agreement indicated between the result obtained from the dipole theory and those obtained in other ways[6] is apparent rather than real.

[5] Cohn, J. Biol. Chem. **63**, 721 (1925).

[6] Cohn, J. Biol. Chem. **63**, 721 (1925); Biltz, Zeits. f. phys. Chem. **91**, 705 (1916).

This difficulty of a low molecular or particle weight resulting from the application of the dipole theory is to be expected if results published from other laboratories are considered. To mention a single example Wyman[7] has made much more complete and more exact dielectric constant measurements on solutions of the protein zein dissolved in 70 percent n-propyl alcohol over a temperature interval from 0° to 80° and at wave-lengths from 4 to 260 meters. The data show the presence of anomalous dispersion in a convincing manner. In discussing the question of the relaxation time Wyman states "It was calculated on the basis of Stokes' formula that the relaxation time of a spherical molecule of the size of zein (gram molecular weight 100,000) in a medium of viscosity 0.01 ought to be 8×10^{-8} sec. The relaxation times, 2.8×10^{-8} and 5.4×10^{-8} just computed by the Debye theory from the experimental results both correspond to viscosities considerably greater than this, but since relaxation time and viscosity are proportional to one another they may be reduced for comparison. By multiplying 2.8×10^{-8} by 0.010/0.017 and 5.4×10^{-8} by 0.010/0.034 (the fractions being appropriate viscosity ratios) we obtain respectively 1.7×10^{-8} and 1.6×10^{-8}." Both of these values are about $\frac{1}{5}$ of that calculated by the theory by assuming $G_2=100{,}000$ and using the proper mathematical relationship, which means that any molecular weight calculated from these data will be too small by the same factor. The data themselves seem to be at least as good as any which have been reported to date for a protein in a solvent.

Two outstanding difficulties which must be overcome before Eq. (14) may be applied to the determination of a particle size or weight are given below. Because of them and because of lack of knowledge of the proper shape factor to use in connection with the orienting particle a really quantitative result has not as yet been obtained for any system in which the frequency variation of the dielectric constant is involved. When and only when these difficulties can be overcome will it be possible to determine a particle size or weight of true significance.

1. The ordinary macroscopic coefficient of viscosity does not seem to measure the resistance to the orientation of the suspended or dissolved particles. Instead there must be used what might be termed a microscopic viscosity. This is especially true when substances having larger molecules are used as solvent media for smaller molecules.

2. The development of the theory is such that nonpolar suspension or solution media are required for a quantitative interpretation of the results either in terms of the size or electric moment of the suspended particle. Thus the application of the Debye theory to experiments made in polar solvent media will always be of highly questionable significance.

It is interesting in this connection that Wyman extended his measurements to the gels which formed when the zein systems were allowed to stand. No change was observed in the dielectric constant as the gelation took place. The suggestion was made by him that the effective viscosity of the gels with

[7] Wyman, J. Biol. Chem. **90**, 443 (1931).

respect to the rotation of the particles is not the ordinary viscosity entering the simple Stokes' expression. This failure of the dielectric constant to change on gelation reminds one of the corresponding failure of the electrical conductance of a salt solution containing gelatin to change to an appreciable extent when the system sets.

The difficulty involved in the determination of the proper viscosity to use in the formula for the time of relaxation, and therefore for the molecular weight, has already been mentioned. We have even suggested that the theory might well be used to determine the true inner friction constant of a liquid, providing care is taken in the choice of system used. The system studied must conform to the assumptions which have been made in the development of the Clausius-Mosotti law, that is, the second difficulty mentioned above.

Recent experiments with systems in which both rosin oil and castor oil molecules have been dissolved in various hydrocarbons indicate that the time of relaxation for these molecules may be practically independent of the macroscopic viscosity of the solution or solvent as measured with a rotating cylinder viscometer. In other cases where vaseline-like substances have been added to increase the viscosity of the solution anomalous effects have been observed. These results will be presented in another place.

The frequency-dielectric constant curves make it possible to distinguish quite readily between a monodisperse and a polydisperse system. In the case of the polydisperse system the dielectric constant change is a very gradual one, spread out over a considerable range of frequencies, but for the monodisperse system the change from the high value to the low value should be quite sharp. Recent work of Kitchin[8] on rubber systems gives definite indication of an electrical inhomogeneity, which may or may not be accounted for on the basis of a dipole mechanism. The same thing is true of work by Race[9] on the high-frequency electrical properties of insulating oils, in which the change in the dielectric constant appears to represent the sum of the contributions of particles of several sizes. The average size of the particle radius as calculated by Race is 3.4×10^{-8} cm, a value which must be too small by a considerable factor. It may be remarked that a number of the suspended particles in these oils can be seen to scatter light when observed in the ultramicroscope. Such particles should have radii at least eight to ten times as large. It may also be mentioned that no correlation was observed between the change in the viscosity of the oils and the frequency region in which the anomalous dispersion took place.

Summary

The dipole theory of Debye has made it possible not only to learn something about the structures of simpler molecules but also to approximate the size and therefore the weight of a dissolved or suspended molecule or particle. The latter result should follow, as has been pointed out by Marinesco, and

[8] Kitchin, J. Ind. Eng. Chem. **24**, 549 (1932).

[9] Race, Phys. Rev. **37**, 430 (1931); J. Phys. Chem. **36**, 1928 (1932).

also by us, from a study of the time of molecular rotation in an alternating electric field. The method depends upon the fact that because of the frictional resistance of the medium to the rotation of the suspended particles a finite time is required for their orientation in the field. If the frequency dependence of the dielectric constant is determined for a system composed of electrically dissymmetrical particles suspended in a liquid medium there will be found to be a region in which the dielectric constant decreases as the frequency is increased. The theory expresses the size and therefore the weight of the suspended particle in terms of the observed critical frequency and the "viscosity" of the medium.

It is shown that the theory as used by Marinesco can give only an approximate result for a molecular weight. The exact theory of Debye is developed only to the extent which we believe to be necessary to demonstrate this fact. In addition we have considered the changes necessary to the treatment of Debye to make it applicable to the type of binary mixture which must be used in the experimental work. The data now available in the literature are as yet insufficient for the exact determination of the particle size because the systems involved fail to conform to the assumptions underlying either the law of Stokes or the Clausius-Mosotti relation. Nevertheless, calculations from them indicate that once it becomes possible to evaluate the true inner friction constant of the system important results may be obtained. The method readily distinguishes monodisperse and polydisperse sols.

Note added in proof: Since this article was submitted, Bloch and Errera have published an article in *Phys. Zeits.* **33,** 757 (1932) in which they come to much the same conclusions that we have.

Capillary Action in Impregnated Paper Insulation

By J. B. WHITEHEAD AND E. W. GREENFIELD
School of Engineering, Johns Hopkins University

(Received October 11, 1932)

The capillary rise of oil in vertical strips of impregnated paper obeys the same law as the rise of liquids in capillary tubes of circular cross section. From the viscosity and surface tension of an oil and its rate of rise in a given paper, it is possible to compute the "effective capillary radius" of the capillary pores of the paper. The rate of rise in a calibrated paper affords a convenient means of measuring the surface tension when the viscosity of the liquid is known. The rate of penetration of an oil into a paper is directly proportional to the "penetrativity" of the oil as defined in the theory of capillary action. The penetrativities of nine insulating oils and the effective capillary radii of seven different papers have been determined. A uniform relationship between the effective capillary radius and the Gurley air resistance of the paper is indicated.

IN THE course of a study of the electrical properties of impregnated paper as related to the impregnating process, a series of observations was made of the rate of capillary rise of a number of oils in vertical strips of several types of paper. It was found in every case that the rise was accurately proportional to the square root of the time, over the interval studied, 1 hour to 100 hours.

The paper strips, 2.54 cm wide, were mounted vertically, with their lower ends dipping in the oils, and placed in a constant temperature box provided with a glass window. The progressive rise of the level of oil saturation was read with a cathetometer. Fig. 1 shows the results when using a well-known wood pulp paper, 0.004″ thick, as used for cable insulation, and a number of different oils. Some of the constants of the oils are given in Table I. Fig. 2 shows the results on a number of different papers (see Table II) with one type of oil.

TABLE I. *Physical properties of cable oils. August, 1932.*

Oil	Pour point °C	Flash point °C	Specific gravity 40°C	Viscosity in poises 40°C	Viscosity in poises 100°C	Surface tension dynes/cm 40°C	Penetrative power in kraft paper cm-sec. $\times 10^{-3}$ 40°C	Conductivity mhos/cc $\times 10^{-14}$ 40°C
100	35.0	274	0.8788	7.5	0.235	51.8	5.57	34.2
101	15.7	296	0.881	5.7	0.258	31.2	5.0	218.0
102	−7.0	288	0.9268	7.2	0.27	20.1	3.55	1065.0
104	0.0		0.83	0.132	0.0295	32.0	33.0	1.0
105	−7.0	282	0.8829	4.9	0.265	31.3	5.47	84.8
106	4.4		0.935	17.5	0.446	21.6	2.28	149.0
107	4.4	263	0.903	4.07	0.22	38.3	6.52	8.08
108	−29.0	148	0.8805	0.1602	0.027	28.2	28.2	24.8
109	−6.7	271	0.9015	2.46	0.155	33.0	7.67	22.0

TABLE II. *Physical properties of cable papers. June, 1932.*

Kind of paper	Air resistance Gurley seconds	App. specific gravity	Effective capillary radius cm-sec. $\times 10^{-3}$ at 26.4°C	Penetrative power of oil No. 109 cm-sec. $\times 10^{-3}$ 26.4°C.
8 mil low density	100	0.82	1.072	7.63
8 mil high density	180	0.88	0.987	6.25
5 mil high density	290	0.90	0.9325	5.77
4 mil kraft	640		0.816	4.42
8 mil super calendered	640	1.07	0.783	4.07
6.5 mil super calendered	1300	1.13	0.7465	3.7
5 mil super calendered	1900	1.13	0.6975	3.235

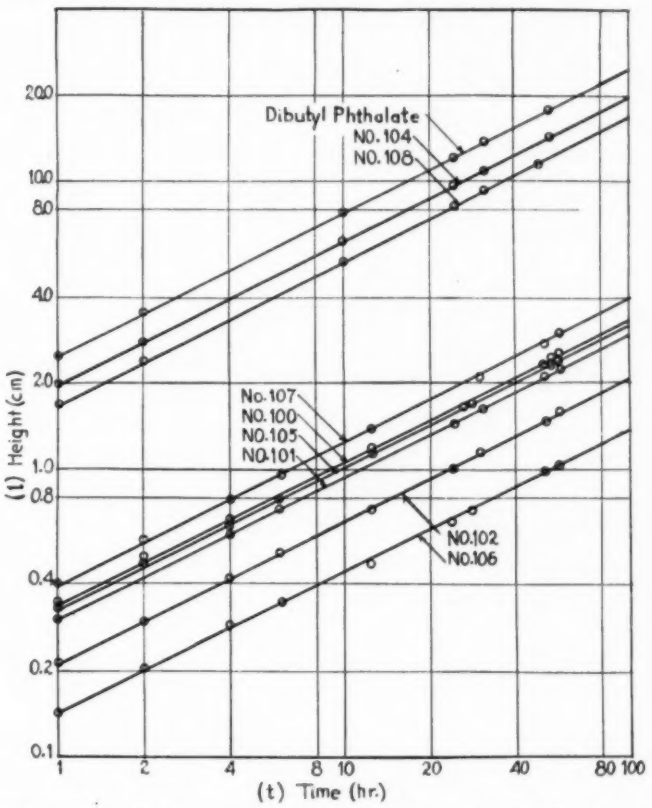

Fig. 1. Penetration study. Kraft paper immersed in various oils. Height-time curves at 40°C, March, 1932. $l = Kt^{1/2}$. K = penetrative power = $(r/2)^{1/2} \cdot (y/\eta)^{1/2}$.

The uniform relation:

$$l = Kt^{1/2} \tag{1}$$

shown in these curves is the same as that found for the rise of liquids in small capillary tubes of circular cross section. This relation is also accounted for in the theory of capillary action. For a straight vertical tube of radius r, Washburn[1] gives

[1] Washburn, Phys. Rev. **17**, 273 (1921).

$$l^2 = [(y/\eta)(\cos\theta/2)]rt \tag{2}$$

and

$$(dl/dt) = (r/\eta)(y/4l)\cos\theta \tag{3}$$

in which l = height of rise, y = surface tension, η = viscosity of the liquid, and θ is the angle between the inner surface of the tube and the meniscus of the liquid ($\theta = 0$ if the liquid wets the tube). It is also shown by Washburn that for very small values of r, θ may always be taken as 0. In these expressions the negative (downward) hydrostatic pressure due to the small values of l is neglected as compared with the capillary (upward) force ($= (2y/r)\cos\theta$).

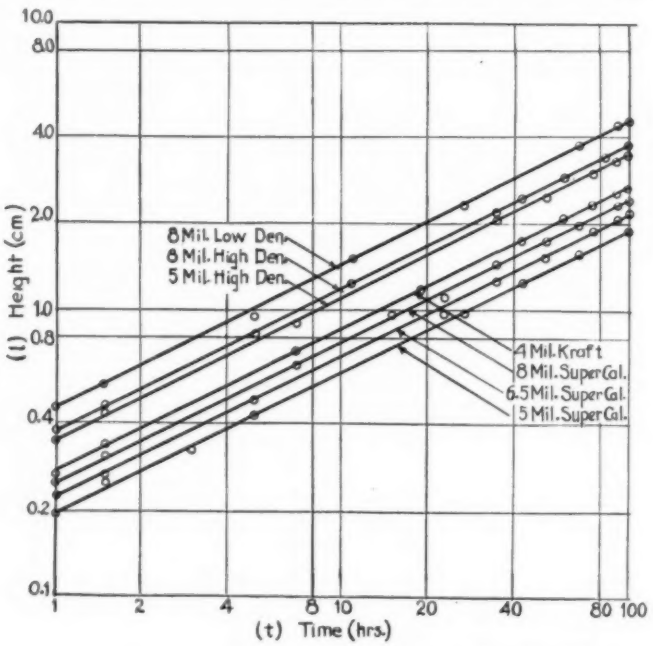

Fig. 2. Penetration study. Various papers immersed in oil. No. 109. Height-time curves at 26.4°C, June, 1932. $l = Kt^{1/2}$. K = penetrative power = $(r/2)^{1/2} \cdot (y/\eta)^{1/2}$.

The quantity $[(y/\eta)\ (\cos\theta)/2)]$ is called the "penetrativity" of the liquid; it is seen to be equal to the square of the distance the liquid rises in a tube of unit radius in unit time. For convenience we will use the constant K of formula (1) in the discussion of our results, and will call it the "penetrating power." The penetrating power involves the radius of the tube as well as the properties of the liquid, and so refers to the penetration of a particular liquid into a particular tube or paper.

We note then that the expression $l = Kt^{1/2}$ applies to a single fine straight capillary tube and also to the mesh of fine capillaries making up the paper strip. For the tube, the penetrating power,

$$K = [(yr/\eta)(\cos\theta/2)]^{1/2} \tag{4}$$

or, for small tubes, $\theta = 0$,

$$K = \left(\frac{yr}{2\eta}\right)^{1/2} = \left(\frac{r}{2}\right)^{1/2} \cdot \left(\frac{y}{\eta}\right)^{1/2}. \tag{5}$$

In these values of K the only factor peculiar to the tube is its radius r, y and η being the surface tension and the viscosity, respectively, of the impregnating liquid.

Obviously, owing to the complexities of structure of the cellulose fibers in a paper tape, it is not permissible to assume that the various factors governing the rate of rise of a liquid in a vertical strip enter in the same way as in the case of a capillary tube. Nevertheless, the identity of the experimental relation in the two cases is very striking, and it is immediately obvious that with a given liquid and paper there is a particular value of r for each paper, which enables us to compute the rise of an impregnating liquid in the paper by using the same Eq. (2), which applies to a straight capillary tube. We may call this value of r the "effective capillary radius" of the paper. The value of the effective capillary radius is readily computed from the values of K as found experimentally, if the values of y and η are known.

The values of η, the viscosity, are usually available or readily measured for any insulating oil. However the values of y, the surface tension, are by no means so easy to obtain, doubtless owing to the difficulty of accurate measurement for liquids of the high values of viscosity pertaining to insulating oils: for viscosities above 2 poises, static methods are subject to serious error. We have met this difficulty by making direct measurements of y and η on two of the lightest oils studied and also on dibutyl phthalate. The last named liquid is practically non-volatile under ordinary conditions (hence is closely similar to the oils), and the values of y and η are given in the International Critical Tables; our own measurements (Saybolt apparatus for η, and Jolly balance for y) were in good agreement. In this way we were able to compute the effective capillary radius for any paper with three different liquids, and so "calibrate" the paper for the measurement of y for any oil for which η was known. In the case of a low viscosity insulating oil, the value of surface tension as measured by the penetration of the oil into a calibrated paper agreed within 2 percent with the value obtained by a series of measurements on a precision Jolly balance.

We thus have a convenient indirect method for measuring the surface tension of the heavier viscous liquids, in the rate of rise in a capillary tube or in a calibrated paper. This method is so simple that it appears probable that others have used it.

Table III gives the values of surface tension and of viscosity as measured at three temperatures for dibutyl phthalate, and for oils No. 104 and No. 108, both thin water-white oils of the type used in oil-filled cables. The table also gives the values of K (cm and sec.) and the corresponding computed values for r the effective capillary radius of the 4 mil kraft paper. It will be noted that r is of the order of magnitude 10^{-5} cm, and that the value is fairly constant as based on measurements with different oils and different lengths of the same paper. However, r increases markedly with increase of tempera-

TABLE III. *Capillary calibration of 4 mil kraft paper. June, 1932.*

Property	Temperature of the Measurement						
	Comp. No. 104			No. 108	Dibutyl phthalate		
	24°C	40°C	60°C	24°C	23°C	40°C	60°C
Specific gravity	0.84	0.83	0.818	0.891	1.044	1.0307	1.015
Viscosity (η) in poises	0.26	0.132	0.073	0.34	0.178	0.0905	0.054
Surface tension dynes/cm (γ)	33.45	32.0	30.27	30.0	36.9	35.5	33.5
Penetrative power cm-sec. $\times 10^{-3}(K)$	23.7	33.0	45.8	18.83	28.85	41.2	50.3
Eff. capillary rad. cm $\times 10^{-5}$ (r)	0.875	0.899	1.011	0.804	0.801	0.867	0.821

TABLE III. (*Continued*). *Effective capillary radius of 4 mil kraft paper.**

24°C	40°C	60°C
0.816×10^{-5} cm	0.882×10^{-5} cm	0.916×10^{-5} cm

* Note: Computed from average values of the penetrative power of three different liquids into 4 mil kraft paper.

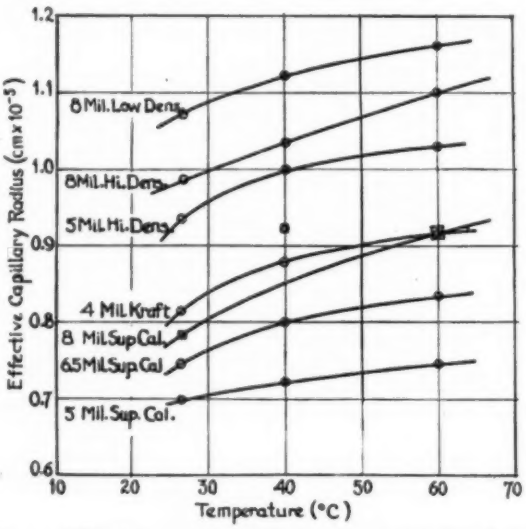

Fig. 3. Effective capillary radius *vs.* temperature. Seven different papers, July, 1932.

ture presumably due to volumetric expansion. Fig. 3 shows the effect of temperature upon the value of the effective capillary radius for several different papers.

Table II gives the values of the effective capillary radius for a number of different grades of paper. The papers are arranged in the order of increasing air resistance. The influence of increased density and of super-calendering on the air resistance is readily seen. The fourth column of Table II, gives the effective capillary radius, computed as indicated above, from measurements of the capillary rise of oil No. 109. It is seen that the effective capillary radius decreases uniformly through the entire group, with increasing air resistance.

The fifth column of the table gives the value of the penetrating power of oil No. 109 into the various papers and the same uniform correlation with the

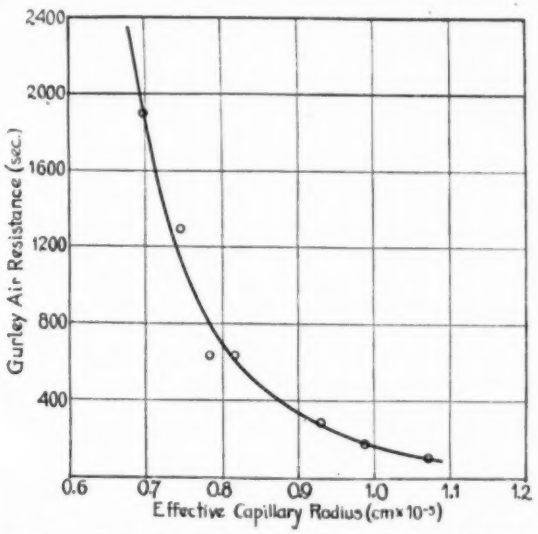

Fig. 4. Effective capillary radius *vs.* Gurley air resistance 26.4°C, July, 1932.

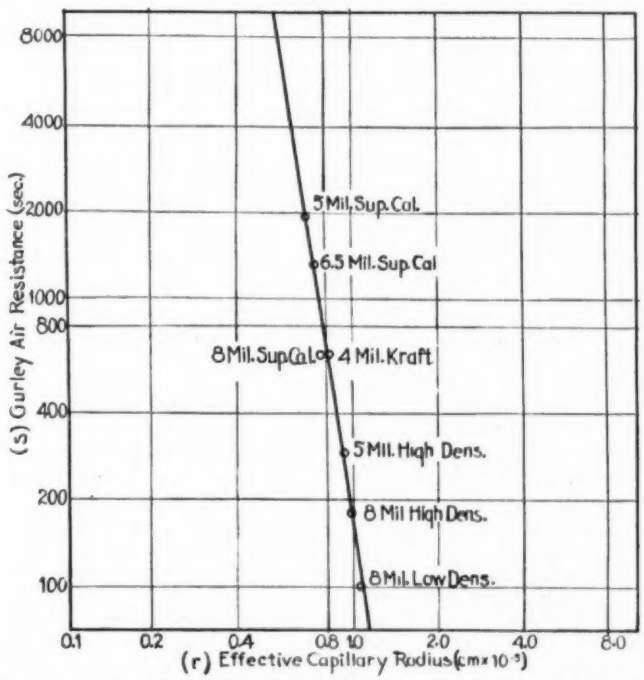

Fig. 5. Effective capillary radius *vs.* Gurley air resistance 26.4°C, July, 1932.
$\log S = \log k - n \log r$. $n = 6.5$. $S = k(1/r)^{6.5}$.

air resistance is evident. The relation between air resistance and effective capillary radius is shown graphically in rectangular coordinates in Fig. 4, and

in Fig. 5 the same data are plotted in double logarithmic coordinates. The straight line of the double logarithmic record indicates the Gurley air resistance of the paper is inversely proportional to the 6.5th power of the effective capillary radius. There is no obvious explanation of this relationship. If the longitudinal capillary channels were of the same type as the transverse air channels, the inverse air resistance should be proportional to the square of the effective capillary radius. The appearance of the 6.5th power makes it evident that the two types of channel are widely different. A wide variation in air resistance is accompanied by a much smaller variation in capillary radius. Increased density and super-calendering have a much greater influence on air resistance than on capillary radius. Apparently the capillary properties arise in the narrow passages at the surfaces of contact of the cellulose fibers all compressed in the plane of the paper, while the air resistance obviously depends on the transverse density of the mesh as well as on the surface conditions. The two types of passage are obviously different, and were it not for the definite relation suggested by Fig. 5, one might readily conclude that the capillary and impregnating properties of a paper are more or less independent of the air resistance. That some connection exists however, seems to be definitely indicated by the clean cut relation of Fig. 5.

Further studies are under way as to possible relationships between the penetrating power of the oil, the capillary properties of the paper, and the electrical properties and behavior of the impregnated paper.

Acknowledgment

These studies have been carried out with the cooperation and support of the Underground Systems Committee of the National Electric Light Association, to whom cordial acknowledgment is hereby made. Thanks are also extended to Messrs. C. O. Newman and C. E. Young for assistance in the experiments.

AUTHOR INDEX TO VOLUME 3

References with (EC) are from the Editor's Column

Allen, S. J. M., H. Kersten and Joseph Maas. Crystal structure of electrodeposits from copper acetate solutions—169

Ambrose, H. A. (see Lawton, H. C.)—185

Anderson, Evald. On the role of the electric wind in electrical precipitation in gases—23

Austin, J. B. Temperature distribution in solid bodies during heating or cooling. A correction—179

——— Vacuum apparatus for measuring thermal expansion at elevated temperatures, with measurements on platinum, gold, magnesium and zinc—240

Barret, William M. Semiportable alternating-current susceptibility meter—149

Barton, Donald C. Eötvös torsion balance—29

Barton, H. A. Atomic disintegration by artificially accelerated protons—159(EC)

Berberich, Leo J. Measurements of the phase angles of shielded resistors—296

Bleakney, William M. Some measurements on the vapor viscosities of the two common pentanes, two pentenes, and carbon tetrachloride—123

Botset, H. G. (see Wyckoff, R. D.)—90

Buchta, J. W. Auditory mechanism—203(EC)

——— Magneto-optical method of chemical analysis—54(EC)

Cameron, G. Harvey. X-ray method of determining the sizes of sub-microscopic crystals—57

Campbell, George A. Three superfluous systems of electromagnetic units—230

Cole, Kenneth S. Theory of surface conductance at an electrolyte-solid interface—114

Dickinson, T. M. (see Metcalf, G. F.)—11

Gaines, Newton. Magnetostriction oscillator producing intense audible sound and some effects obtained—209

Greenfield, E. W. (see Whitehead, J. B.)—324

Hanawalt, J. D. (see Morell, L. G.)—161

Heiland, C. A. Preliminary note on a new magnetometer—18

Hill, E. L. Interaction of light and sound waves—119(EC)

——— Mass of the hydrogen isotope H^3—268(EC)

——— Quantum mechanics and optics—120(EC)

——— Relativistic quantum mechanics—269(EC)

——— Wave nature of atoms—268(EC)

Kersten, H. (see Allen, S. J. M.)—169

——— and Joseph Maas. Crystal structure of black nickel—137

Koga, Isaac. Thickness vibrations of piezoelectric oscillating crystals—70

Lawton, H. C., H. A. Ambrose and A. G. Loomis. Chemical treatment of rotary drilling fluids. Release of cuttings: Chemical *vs.* mechanical methods—185

Loomis, A. G. (see Lawton, H. C.)—185

Maas, Joseph (see Allen S. J. M.)—169

——— (see Kersten, H.)—137

McDermott, Eugene. Application of the reflection seismograph—39

Metcalf, G. F. and T. M. Dickinson. New low noise vacuum tube—11

Morell, L. G. and J. D. Hanawalt. X-ray study of the plastic working of magnesium alloys—161

Morgan, S. O. (see White, A. H.)—53

Muskat, M. (see Wyckoff, R. D.)—90

Oncley, J. L. (see Williams, J. W.)—314

Osteen, John A. Resistance-temperature relation of beryllium oxide and zinc oxide—81

Peters, J. C., Jr. and E. B. Woodford. Characteristics of certain caesium-oxide photoelectric cells—172

Poulter, Thos. C. and Lester Uffelman. Penetration of hydrogen through steel at four thousand atmospheres—147

Slichter, Louis. Theory of the interpretation of seismic travel-time curves in horizontal structures—273

Smith, W. O. Capillary flow through an ideal uniform soil—139

Thompson, L. Reduced scale studies in armor penetration—155

Uffelman, Lester (see Poulter, Thos. C.)—147

Waldorf, Sigmund K. Amplifier-oscillograph applied to the study of dielectrics with continuous potentials—1

Westendorp, W. F. Inverter-lamp for the conversion of 60-cycle power into 1000-cycle modulated light —193

Wetzel, W. W. Quantum mechanics and collision problems—205(EC)

White, A. H. and S. O. Morgan. Erratum: Dielectric properties of some glycols—53

Whitehead, J. B. and E. W. Greenfield. Capillary action in impregnated paper insulation—324

Williams, J. W. and J. L. Oncley. Dielectric constant and particle size—314

Woodford, E. B. (see Peters, J. C.)—172

Wyckoff, R. D., H. G. Botset, M. Muskat. Flow of liquids through porous media under the action of gravity—90

ANALYTIC SUBJECT INDEX TO VOLUME 3

Alloys
X-ray study of the plastic working, L. G. Morell, J. D. Hanawalt—161

Armor
Reduced scale studies in penetration, L. Thompson— 155

Capillary action
Flow of liquids through porous media, R. D. Wyckoff, H. G. Botset, M. Muskat—90
Flow through an ideal soil, W. O. Smith—139
In impregnated paper insulation, J. B. Whitehead, E. W. Greenfield—324

Conductivity, electrical (see Electrical conductivity and resistance)

Conductivity, thermal (see Heat conduction)

Crystals and crystal structure
Changes in structure of black Ni, H. Kersten, J. Maas—137
Sizes of sub-microscopic crystals by x-rays, G. H. Cameron—57
Structure of electrodeposits from coppper acetate solutions, S. J. M. Allen, H. Kersten, J. Maas—169
Thickness vibrations of piezoelectric oscillating crystals, I. Koga—70
X-ray study of the plastic working of alloys, L. G. Morell, J. D. Hanawalt—161

Dielectrics and dielectric properties
Amplifier-oscillograph; dielectrics with continuous potentials, S. K. Waldorf—1
And particle size, J. W. Williams, J. L. Oncley—314
Properties of some glycols, A. H. White, S. O. Morgan—53

Drilling fluids
Chemical *vs.* mechanical methods of treatment of rotary drilling fluids, H. C. Lawton, H. A. Ambrose, A. G. Loomis—185

Editor's column
Atomic disintegration by artificially accelerated protons, H. A. Barton—159
Auditory mechanism, J. W. Buchta—203
Chemical analysis by magneto-optical method, J. W. Buchta—42
Interaction of light and sound waves, E. L. Hill—119
Mass of the H isotope H^2, E. L. Hill—268

Editor's column (continued)
Quantum mechanics and collision problems, W. W. Wetzel—205
Quantum mechanics and optics, E. L. Hill—120
Relativistic quantum mechanics, E. L. Hill—269
Wave nature of atoms, E. L. Hill—268

Electrical circuits
Inverter-lamp for 1000-cycle modulated light; 60-cycle power, W. F. Westendorp—193

Electrical conductivity and resistance
Conductance at an electrolyte solid interface, K. S. Cole—114
Resistance-temperature relation of oxides, J. A. Osteen—81

Errata
Dielectric properties of some glycols, A. H. White, S. O. Morgan—53
Temperature distribution in solids during heating or cooling, J. B. Austin—179

Gases
Penetration of H through steel, T. C. Poulter, L. Uffelman—147

Geophysics
Application of the reflection seismograph, E. McDermott—39
Capillary flow through an ideal soil, W. O. Smith—139
Flow of liquids through porous media, R. D. Wyckoff, H. G. Botset, M. Muskat—90
Seismic travel-time curves in horizontal structures, L. Slichter—273
Semiportable susceptibility meter, W. M. Barret—149
Use of Eötvös torsion balance, D. C. Barton—29

Heat conduction
Temperature distribution in solids during heating, J. B. Austin—179

Instruments and methods
Amplifier-oscillograph; dielectrics with continuous potentials, S. K. Waldorf—1
Application of the reflection seismograph, E. McDermott—39
Electric wind in electrical precipitation in gases, Evald Anderson—23
Eötvös torsion balance, D. C. Barton—29
Inverter-lamp for 1000-cycle modulated light; 60-cycle power, W. F. Westendorp—193

Instruments and Methods—(continued)
Magnetostriction oscillator producing intense audible sound, N. Gaines—209
Measurements on vapor viscosities, W. M. Bleakney—123
New low noise vacuum tube, G. F. Metcalf, T. M. Dickinson—11
New magnetometer, C. A. Heiland—18
Penetration of H through steel, T. C. Poulter, L. Uffelman—147
Phase angles of shielded resistors, L. J. Berberich—296
Semiportable susceptibility meter, W. M. Barret—149
Sizes of sub-microscopic crystals by x-rays, G. H. Cameron—57
Thermal expansion at elevated temperatures, J. B. Austin—240
Treatment of rotary drilling fluids, H. C. Lawton, H. A. Ambrose, A. G. Loomis—185

Insulation
Capillary action in impregnated paper insulation, J. B. Whitehead, E. W. Greenfield—324

Liquids
Capillary flow through an ideal soil, W. O. Smith—139
Conductance at an electrolyte solid interface, K. S. Cole—114
Flow through porous media under the action of gravity, R. D. Wyckoff, H. G. Botset, M. Muskat—90

Oscillators
Magnetostriction oscillator producing intense audible sound, N. Gaines—209

Photoelectric effect; cells
Characteristics of CsO cells, J. C. Peters, Jr., E. B. Woodford—172

Piezoelectric properties
Thickness vibrations of crystals, I. Koga—70

Precipitators
Electric wind in electrical precipitation in gases, E. Anderson—23

Sound
Magnetostriction oscillator producing intense audible sound; some effects, N. Gaines—209

Steel
Armor penetration, L. Thompson—155
Penetration by H, T. C. Poulter, L. Uffelman—147

Thermal expansion
At elevated temperatures, results on Pt, Au, Mg and Zn, J. B. Austin—240

Units
Superfluous systems of electromagnetic units, G. A. Campbell—230

Vacuum tubes
Low noise tube, G. F. Metcalf, T. M. Dickinson—11

Viscosity
Measurements on vapor viscosities, W. M. Bleakney—123